# Loss of mitochondrial proline catabolism depletes FAD, impairing sperm function, and male reproductive advantage

Chia-An Yen[,1,2], Dana L. Ruter[3], Nathan Mih[4], Shanshan Pang[5], and Sean P. Curran[1,2,5,6*]

1. Leonard Davis School of Gerontology, University of Southern California, Los Angeles, CA 90089
2. Department of Molecular and Computation Biology, Dornsife College of Letters, Arts, and Sciences, University of Southern California, Los Angeles, CA 90089
3. Biology Department, Integrative Program for Biological and Genome Sciences, University of North Carolina, Chapel Hill, NC 27599
4. Department of Bioinformatics and Systems Biology, University of California San Diego, La Jolla, CA 92093
5. School of Life Sciences, Chongqing University, Chongqing 401331, China.
6. Norris Comprehensive Cancer Center, Keck School of Medicine, University of Southern California, Los Angeles, CA 90089

Correspondence to: spcurran@usc.edu

**KEYWORDS**

spermatogenesis, mitochondria, germ cells, reproduction, proline catabolism, alh-6/ALDH4A1, C. elegans, senescence, aging, male-specific

**ABSTRACT**

Exposure to environmental stress has a clinically established influence on male reproductive health, but the impact of normal cellular metabolism on sperm quality and function is less well-defined. Here we show that homeostatic changes in mitochondrial dynamics driven by defective mitochondrial proline catabolism result in pleiotropic consequences on sperm quality and competitive fitness. Disruption of *alh-6*, which converts 1-pyrroline-5-carboxylate (P5C) to glutamate, results in P5C accumulation that drives oxidative stress, activation of SKN-1, and a reduction of energy-storing flavin adenine dinucleotide (FAD) levels. These molecular changes lead to premature male reproductive senescence by reducing sperm quality. These sperm-specific defects are suppressed by abating P5C metabolism, by treatment with antioxidants to combat reactive oxygen species (ROS), or by feeding diets that restore FAD levels. Our results define a role for mitochondrial proline catabolism and FAD homeostasis on sperm function and specify strategies to pharmacologically reverse unintended outcomes from SKN-1/Nrf transcriptional activation.

## INTRODUCTION

As individuals wait longer to have families, reproductive senescence has become an increasingly prudent topic (1, 2). Decline in oocyte quality is well-documented with age and can result in fertility issues when older couples try to conceive (3). Furthermore, pregnancies at an older age pose risks for higher incidences of birth defects and miscarriages. In humans, female reproduction ceases at menopause at an average age of 41-60, with the onset of menopause (4). The *C. elegans* "wild type" is hermaphroditic and self-fertilizing; however, they are capable of making and maintaining Mendelian ratios of male (sperm-only) animals in their populations. Like humans, *C. elegans* experience a decline in fecundity with age by halting oocyte production at roughly one-third of their lifespan (5). In addition, regulators of reproductive aging insulin/IGF-1 and *sma*-2/TGF-β signaling are conserved regulators of reproductive aging from worms to human (6). While the majority of studies in reproductive senescence have focused on maternal effects, male factors contribute to a large portion of fertility complications with increasing evidence of an inverse relationship between paternal age and sperm health (2). In fact, studies in mammals have shown an age-related decline in sperm quality with increased incidences of DNA damage, reduced motility, abnormal morphology, and decreased semen volume (7-9).

Mitochondria are essential for their role in creating energy that fuels all cellular functions; however, this process generates reactive oxygen species (ROS) as a byproduct. Low levels of ROS have an important role in cell signaling, hypoxia adaptation, aging, autophagy, immunity, and cell differentiation (10, 11); while high levels of ROS can be detrimental to cellular function and can lead to cell death. Multiple studies in humans and mice have implicated different aspects of mitochondrial function in sperm quality including: mitochondria ultrastructure (12, 13), mitochondrial genome and copy number (14-18), mitochondria protein levels (19-21), and enzyme activity of ETC complexes (22-24). While all these studies imply that mitochondrial integrity and activity are important for proper sperm function, the mechanism behind this relationship is unclear.

Mammalian sperm require a low amount of ROS for multiple aspects of sperm function and successful fertilization of an egg, including: capacitation, hyperactivation, acrosome reaction, and sperm-oocyte fusion (25-27). Interestingly, many studies have found elevated ROS in sperm to be associated with lipid peroxidation, DNA damage, reduced motility, and reduced viability in sperm; although the source of ROS and the mechanism behind ROS-induced sperm defects are unknown (28, 29). Recent studies show that mitochondria-generated ROS through inhibition of electron transport chain results in spermatozoa with reduced motility and lipid peroxidation *in vitro* (30, 31). Since the level of ROS in semen increases with age (7), understanding ROS-mediated sperm defects can provide insight into male reproductive senescence.

Several studies have documented fertility defects in *C. elegans* mitochondrial mutants. Mutation in *nuo-1*, a complex I component of the mitochondria respiratory chain, results in reduced brood size caused by impaired germline development (32). Similarly, *clk-1* mutation affects the timing of egg laying, resulting in reduced brood size (33). Both of these mitochondrial mutations impact fertility, but their role(s) in spermatogenesis are unclear. *alh-6*, the *C. elegans* ortholog of human *ALDH4A1*, is a nuclear-encoded mitochondrial enzyme that functions in the second step of the proline metabolism pathway, converting 1-pyrroline-5-carboxylate (P5C) to glutamate (34). We previously revealed that *alh-6(lax105)* loss-of-function mutants display altered mitochondrial structure in the muscle accompanied by increased level of ROS in adult animals (35). Furthermore, mutation in *alh-6* results in the activation of SKN-1/NRF2 (36), an established regulator of oxidative stress response, likely through the accumulation of toxic P5C disrupting mitochondrial homeostasis (35-39). Interestingly, SKN-1 was recently shown to respond to accumulation of damaged mitochondria by inducing their biogenesis and degradation through autophagy (40). Here, we identify a genetic pathway for regulating male reproductive decline stemming from perturbation of mitochondrial proline metabolism leading to redox imbalance, cofactor depletion, and altered mitochondria dynamics; all of which play a part in sperm dysfunction.

## RESULTS

### Mutation in mitochondrial *alh-6* results in diet-independent reduction in fertility

Altered mitochondrial structure and function have been correlated to loss of proper sperm function in different species (16, 41-43). In addition, proper sperm function requires a low level of ROS (25-27), although a specific role for endogenous mitochondrial derived ROS is undefined. ALH-6/ALDH4A1, is a nuclear-encoded mitochondrial enzyme that functions in the second step of proline catabolism, converting 1-pyrroline-5-carboxylate (P5C) to glutamate (Figure S1). We anticipated that mutation of *alh-6* may affect the germline, based on our previous assessment of the premature aging phenotypes in somatic cells in *alh-6* mutants (35). Using an UV-integrated *alh-6::gfp* strain under its endogenous promoter, we saw that *alh-6* is localized to the mitochondria in the germline of hermaphrodites (Figure S2). We then assessed progeny output of *alh-6(lax105)* hermaphrodites until egg laying ceased and found a reduction in self-fertility brood size (-12.9%) (**Figure 1A**). Since the somatic phenotypes of *alh-6(lax105)* mutants are known to be diet-dependent (35, 36), we examined self-fertility of animals fed the *E. coli* K-12 bacteria HT115, to determine if the reduced reproductive output is also dependent on the type of bacterial diet ingested. Surprisingly, we found that the self-fertility of *alh-6* animals was markedly reduced (-20.7%), when animals were fed the K-12 diet (**Figure 1B**). *alh-6* mutants have similar timing in their progeny output as compared to wild type animals on both diets (Figures S3A-B**)**. Since *alh-6* mutants display normal development and reproductive timing, the progeny deficit is not a result of an attenuated reproductive span which reveals the differential impact of *alh-6* loss in the soma (diet-dependent) (35) and the germline (diet-independent).

### *alh-6* fertility defects are sperm-specific

We noted that *alh-6* mutant hermaphrodite animals laid twice as many unfertilized oocytes as wild type animals over their reproductive-span (**Figure 1C)**, suggesting a loss of sperm function (44-46)**.** It is notable that *alh-6* mutant hermaphrodites lay very few, if any, dead eggs (**Figure 1C**), suggesting that the loss of ALH-6 activity is not lethal. To determine whether the reduced brood size of *alh-6* mutants are due to a general loss of germ cells or a specific defect in oocytes or sperm, we examined the mated-fertility of these animals by mating wild type young adult (day 0-1) males to either wildtype or *alh-6* mutant virgin hermaphrodites (in wild type *C. elegans*, male sperm outcompetes hermaphrodite sperm >99% of the time (47, 48)). We found that the reduced fertility in *alh-6* mutant hermaphrodites is fully rescued by wild type sperm, which confirmed that oocyte quality is not impaired but rather, *alh-6* hermaphrodite sperm is dysfunctional (**Figures. 1D-E**).

To better assess the quality of *alh-6* mutant sperm, we measured the ability of *alh-6* mutant sperm to compete with wild type sperm (49). To differentiate between progeny resulting from mating and progeny that arise from hermaphrodite self-fertilization, we made use of male animals harboring a GFP transgene such that any cross-progeny will express GFP while progeny that arise from hermaphrodite self-sperm will not (**Figure 1D)**. We found that wild type hermaphrodites when mated to *alh-6* mutant males have significantly more self-progeny as compared to wild type hermaphrodites mated to wild type males (**Figure 1F**). This finding indicates a sperm competition deficit of *alh-6* males resulting in a brood derived from self-fertilization, which is uncommon after mating has occurred (47). As hermaphrodite *C. elegans* produce a set amount of sperm during L4 stage before switching exclusively to oogenesis, eventually depleting its reservoir of sperm (47, 50). To assess whether *alh-6* mutant sperm are generally-dysfunctional, we mated older hermaphrodites that had depleted their complement of self-sperm and found that *alh-6* mutant males are able to produce equal numbers of progeny as wild type males when the need for competition with hermaphrodite sperm is abated (Figure S4A); thus, although *alh-6* mutant sperm are impaired for competition, they remain competent for reproduction. This is similar to recent study on *comp-1,* a mutation which results in context-dependent competition deficit in *C. elegans* sperm (51). Similarly, older *alh-6* mutant hermaphrodites mated to young wild type males yield similar level of progeny as age-matched WT hermaphrodites, which further supports a model where sperm, but not oocytes, are defective in *alh-6* mutants (Figure S4B).

Similar to mammals, the contribution of sperm to fertility in *C. elegans* is dictated by distinct functional qualities, which include: sperm number, size, and motility (49, 52, 53). In *C. elegans*, male sperm are larger and faster than hermaphrodite sperm, which affords a competitive advantage (53). We next sought to define the nature of the sperm competition defect in *alh-6* mutants by measuring sperm size, motility, and number in *alh-6* mutants compared to wild type animals. One day after spermatogenesis initiation (at the L4 larval stage of development), *alh-6* adult hermaphrodites have a reduced number of sperm in the spermatheca as compared to wild type (Figure S5A), which is correlated with the reduced self-fertility observed (**Figures 1A-B**). In contrast, age-matched *alh-6* mutant males have similar numbers of sperm as WT males, suggesting that they have a similar rate of production (**Figure 2A**). We next examined sperm size in day 1 adult males and discovered that *alh-6* mutant spermatids are significantly smaller as compared to wild type (**Figure 2B**). To achieve motility, *C. elegans* sperm must be activated to allow pseudopod development, and this development requires protease activation (54) (Figure 5B). *In vitro*, sperm activation can be recapitulated by treatment of isolated spermatids with Pronase (55). In addition to reduced size, the percentage of activated spermatozoa was significantly reduced in *alh-6* mutants as compared to wild type (**Figure 2C**). Taken together, the reduction of sperm quantity and quality (size and activation) are contributors to the reduced fertility in *alh-6* mutants.

**Transcriptional signatures define temporal phenotypes of *alh-6* activity**

We first identified *alh-6* mutant in a screen for activators of the cytoprotective transcription factor SKN-1/NRF2 using *gst-4p::gfp* as a reporter (35, 36). When activated, SKN-1 transcribes a variety of gene targets that collectively act to restore cellular homeostasis. However, this can come with an energetic cost with pleiotropic consequences (35, 36, 56-61). *alh-6* mutants have normal development, but display progeric phenotypes towards the end of the normal reproductive span (35) indicating a temporal switch in phenotypic outcomes. We reasoned that the temporally controlled phenotypes in the *alh-6* mutants could be leveraged to identify potential mechanisms by which *alh-6* loss drives cellular dysfunction. As SKN-1 is activated in *alh-6* mutants after day 2 of adulthood (35), we defined genes that display differentially altered expression in the L4 developmental stage, when spermatogenesis occurs, as compared to Day 3 adults (post SKN-1 activation). We performed RNA-Seq analyses of worms with loss of *alh-6* and identified 1935 genes in L4 stage animals and 456 genes in Day 3 adult animals that are differentially expressed (+/- Log2 (fold change), 0.05 FDR). Intriguingly, the gene expression changes at these two life periods had distinct transcriptional signatures (**Figures 3A-B**; Figure S6). Because the loss of *alh-6* drives compensatory changes in normal cellular metabolism, which later in life results in the activation of SKN-1, we expected to identify significant changes in both metabolic genes and SKN-1 target genes. Supporting this hypothesis, the gene ontology (GO) terms most enriched include oxidoreductases and metabolic enzymes in L4 stage animals (**Figure 3A**) and SKN-1-dependent targets such as glutathione metabolism pathway genes in Day 3 adults (**Figure 3B**). Importantly, our transcriptomic analysis recapitulated the temporally-dependent phenotypic outcomes resulting from *alh-6* loss; genes in the pseudopodium and germ plasm GO terms class displayed reduced expression in L4 (**Figure 3A**), which could impact *C. elegans* spermatogenesis. In contrast, genes in the muscle-specific GO term class displayed increased expression in day 3 adults (**Figure 3B**), which is when SKN-1 activity is enhanced in the muscle of *alh-6* mutants (36). Taken together, the transcriptome analysis of *alh-6* mutants is diagnostically relevant and informative for defining drivers of organism-level phenotypic changes in animals with altered proline catabolism.

**FAD mediates sperm functionality and competitive fitness**

The strong enrichment of genes whose protein products utilize and/or bind cofactors or co-enzymes was intriguing as the maintenance of metabolic homeostasis and the redox state of the cell requires a sophisticated balance of multiple cofactors (**Figure 4A**). In fact, the proline catabolism pathway utilizes multiple cofactors to generate glutamate from proline; PRDH-1 uses FAD as a co-factor while ALH-6 utilizes the reduction of NAD+. In the absence of ALH-6, PRDH-1 would continue to deplete FAD, which would activate compensatory pathways to maintain metabolic homeostasis in addition to

activating pathways to detoxify P5C (oxidoreductases, P5C reductase, etc.). In light of this hypothesis we measured FAD and found a significant reduction in *alh-6* mutant animals (**Figure 4B**). As such, we predicted that restoration of FAD levels might alleviate the sperm-specific phenotypes of *alh-6* mutants. Dietary supplementation of riboflavin has been shown to increase cellular FAD levels (62, 63), and when fed to *alh-6* mutants, it restored sperm function. We found that wild type hermaphrodites mated to *alh-6* mutant males that were fed a diet supplemented with 2.5mM riboflavin produced significantly more total progeny than *alh-6* males fed the standard OP50 diet (Figure S7). Moreover, riboflavin supplementation was sufficient to restore male sperm size (**Figure 4C**) and also rescued the impaired activation (**Figure 4D**) of male sperm in *alh-6* mutants. Taken together, these data suggest that loss of *alh-6* leads to a decrease in cellular FAD levels that drives sperm dysfunction.

**Loss of cellular proline catabolism is not causal for sperm defects in *alh-6* mutants**

We were curious to uncover additional molecular mechanisms that underlie the loss of sperm function in *alh-6* mutants. To do this, we performed an EMS mutagenesis screen to identify suppressors of the induced *gst-4p*::*gfp* expression phenotype in *alh-6* mutants (**Figure 5A**) (35). We identified one suppressor allele, *lax228,* which we mapped to right arm of chromosome IV between F49E11 and Y57G11B SNPs. We then generated a list of candidate genes in this region with non-synonymous mutations in the exons of protein coding genes using whole genome sequencing data of the *alh-6* mutant compared to the suppressor mutant *alh-6(lax105); lax228* (64). We tested each of these genes by RNA interference (RNAi) in the *alh-6;gst-4p::gfp* strain to phenocopy the suppressor. RNAi of *B0513.5,* hereafter referred to as *prdh-1* as it encodes for proline dehydrogenase, was the only RNAi target that phenocopied the *lax228* mutant (Figures S8A-B). PRDH-1 catalyzes the first enzymatic step of proline catabolism (**Figure 5B**), converting proline to P5C. Importantly, this enzyme is linked to several of the phenotypes of *alh-6* mutants including the generation of P5C (*9*) and the continued reduction of FAD, documented above (**Figure 4B**). We also examined the expression of the proline catabolism pathway genes from our RNA-Seq analysis and discovered a significant increase in the expression of enzymes that would prevent the accumulation of P5C in *alh-6* mutant L4 animals, before irreparable damage occurs (**Figure 5C**). Specifically, there was an increase in expression of pyrroline-5-carboxylate reductase (*M153.1/PYCR)* that converts P5C back to proline and ornithine transaminase(*oatr-1/OAT)* that converts P5C to ornithine. Surprisingly, the expression of pyrroline-5-carboxylate synthase (*alh-13/P5CS)* was also increased, however P5CS has two enzymatic functions: glutamate kinase (GK) and γ-glutamyl phosphate reductase (GPR) activities that impact additional nodes of cellular metabolism. Moreover, since proline itself has important roles in cellular protection, the increased expression of P5CS might be an important stress response, but with pleiotropic consequences as it would deplete glutamate and increase an already accumulating pool of P5C.

To determine how the total loss of proline catabolism would affect *C. elegans* reproduction, we examined the *alh-6; prdh-1* double mutant in our panel of reproduction and sperm quality assays. The reduction in spermatid size (**Figure 5D**) and impairment of spermatid activation (**Figure 5E**) in *alh-6* mutants are both suppressed by loss of *prdh-1*. In addition, the *prdh-1* mutation restored the reduced self-fertility (Figure S9A), lower hermaphrodite sperm count (Figure S9B), and suppressed the increased laying of unfertilized oocytes of the *alh-6* single mutant (Figure S9A). Finally, the reduced ability of *alh-6* male sperm to compete against wild type hermaphrodite sperm was abrogated in the *alh-6;prdh-1* double mutant (Figure S9C). These results were surprising as they reveal that loss of flux through the mitochondrial proline catabolism pathway is benign for animal reproductive fitness, but suggests instead that P5C accumulation is instrumental in driving sperm dysfunction in *alh-6* animals.

**Endogenous ROS drives *alh-6* sperm defects**

Several studies have examined the impact of exogenous ROS-inducing electrophiles on sperm function, but the impact of endogenously produced ROS on sperm function remains poorly defined. The continuous generation of P5C by PRDH-1 leads to the accumulation of this highly toxic and unstable biomolecule, which can lead to redox imbalance and impair the normal function of germ cells as it does

for somatic tissues (35, 37-39, 65). If the sperm defects in the *alh-6* mutants are a result of a loss of redox and/or ROS homeostasis, then we anticipated that antioxidants could alleviate these phenotypes. We supplemented the diet of *alh-6* mutant males with the antioxidant N-acetylcysteine (NAC), from birth through reproductive maturity, and re-measured the reproductive parameters of these animals. NAC supplementation restored spermatid size and activation of *alh-6* animals to WT levels (**Figures 5D-E**). Antioxidant supplementation in wild type (Figures S10A-B) or *alh-6; prdh-1* double mutants had no effect (Figures S10C-D). Collectively, these data suggest that endogenous production of ROS is causative for the sperm dysfunction seen in *alh-6* animals. In addition, this study reveals that antioxidant supplementation can act as a treatment to overcome reproductive deficiencies stemming from defects in specific cellular metabolic pathways.

**Mitochondrial dynamics regulate spermatid function**

Although there is a clear and documented role for mitophagy in the clearance of paternal mitochondria post-fertilization in *C. elegans*, the role(s) for mitochondrial dynamics and turnover in sperm function prior to zygote formation are unclear. We first examined mitochondrial dynamics in wild type sperm by staining with the fluorescent, mitochondrial-specific dye JC-1 (ThermoFisher), and noted that each spermatid on average contained multiple discernable spherical mitochondria that are mostly not fused (**Figures 6A, 6B, 6G**). Previous studies in yeast and cultured mammalian cells have shown that when cells are exposed to mild stress, the initial response of mitochondria is to fuse in an attempt to dilute damage (66-68). Indeed *alh-6* mutant spermatids had mitochondria that were more interconnected (**Figures 6C, 6D, 6G**) as compared to wild type spermatids, which supports our finding that these sperm are under oxidative stress (**Figure 5**). Loss of *prdh-1*, which restores sperm function (**Figure 5**), returned spermatid mitochondria to more punctate structures (**Figures 6E, 6F, 6G**). Similarly, treatment with the antioxidant NAC returned *alh-6* mutant mitochondria in spermatids to wild type levels of fusion (**Figure 6H**). The JC-1 dye accumulates in mitochondria in a membrane potential ($\Delta\Psi$)-dependent manner, and as concentration exceeds threshold, its fluorescence switches from green to red emission; thus, a higher red-to-green fluorescence ratio is indicative of healthier mitochondria, with higher $\Delta\Psi$. *alh-6* mutant spermatids have reduced red:green JC-1 fluorescence that indicates a lower mitochondrial $\Delta\Psi$, and an accumulation of unhealthy mitochondria (**Figure 6I**).

The role of mitochondrial dynamics (fusion and fission) in the maturation of sperm has not been studied; however recent work has revealed that the mitochondrial fusion and fission machinery are important for the elimination of paternal mitochondria post-fertilization (69). FZO-1 is required for proper fusion of the mitochondrial membranes and DRP-1 is required for mitochondrial fission (70, 71). The balance of this fusion and fission machinery in the upkeep of mitochondrial homeostasis allows cells to respond to changes in metabolic needs and external stress (72, 73). RNAi of *fzo-1* suppressed the enhanced fusion observed in *alh-6* mutant spermatid mitochondria indicating mitochondrial fusion is active in spermatids with impaired proline catabolism (**Figure 6J**). We next examined spermatids from *drp-1* mutant animals and observed a greater level of mitochondrial fusion as compared to wild type and *alh-6* mutant spermatids (**Figure 6K**). We observed a synergistic level of mitochondrial fusion in spermatids derived from *alh-6; drp-1* double mutants. This finding is consistent with previous studies in yeast which reveal that defects in fusion can be compensated for by changes in the rates of fission and vice versa (72, 73). In support of our model where mitochondrial dynamics act as a major driver of the sperm-specific defects in *alh-6* mutants, we discovered that loss of *drp-1*, which results in increased mitochondrial fusion (like that observed in *alh-6* mutants), also reduces sperm activation (**Figure 6L**). Moreover, reduced *fzo-1* does not alter activation in wild type sperm, but restores activation in *alh-6* sperm (**Figure 6M)**; suggesting increased fusion in *alh-6* sperm mitochondria is impairing proper function. Taken together, these data support a model where loss of mitochondrial proline catabolism induces mitochondrial stress, activating mitochondrial fusion, which can subsequently eliminate damage in order to preserve functional mitochondria (**Figure 6N**). These data also reveal a functional role for mitochondrial fusion and fission in maintaining proper sperm function. In conclusion, our studies define mitochondrial proline catabolism as a critical metabolic pathway for male reproductive health.

## DISCUSSION

Here we investigate the effects of mutation in the mitochondrial enzyme gene *alh-6,* and the associated increased ROS levels on male fertility stemming from defective mitochondrial proline catabolism. We found that *alh-6* mutants show a reduction in brood size that is sexually dimorphic; defects in sperm function but not oocytes contribute to reduced hermaphrodite fertility. As societal factors continue to push individuals to wait longer to have children, our studies are of critical importance to elucidate how restoring and maintaining functional amino acid catabolism during aging will promote reproductive success.

Although *C. elegans* is a well-established organism for studying aging and reproduction, with several studies describing hermaphrodite reproductive senescence, many questions regarding the basis of male reproductive decline remain unanswered. Decades of work have shown that exposure to pollution, toxins, xenobiotics, and other ROS-inducing compounds can prematurely drive the loss of sperm function (29, 74, 75), but the impact that normal cellular metabolism plays on sperm function and the identification of specific molecules that can mediate sperm quality are not well-defined. In this study we characterized a new role for mitochondrial proline catabolism and FAD homeostasis in the maintenance of proper sperm function. Perturbation of this pathway, through mutation of *alh-6/ALDH4A1*, increases ROS, causing metabolic stress and increased mitochondrial fusion in spermatids, which results in impaired sperm function and premature reproductive senescence

Mutation in proline dehydrogenase (*PRODH*) in humans results in hyperprolinemia type I (HPI), while mutation in delta-1-pyrroline-5-carboxylate dehydrogenase (*ALDH4A1/P5CDH*) results in hyperprolinemia type II (HPII). Surprisingly, in *C. elegans*, mutation in upstream proline dehydrogenase gene, *prdh-1,* is able to suppress all the reproductive defects in *alh-6* mutants suggesting that overall reduction in proline catabolism is not causal for the observed reproduction phenotypes. In humans, the diagnosis of HPI and HPII are both through by elevated level of proline in plasma, with addition of high level of P5C in HPII patients. The symptoms of HPI varies on severity depending on the reduction of PRODH activity (type of mutation) and are characterized by neurological, auditory, and renal defects (*53*). Although proline catabolism has not previously been shown to have a direct role in fertility, human fertility studies have shown that the addition of proline in cryopreservation medium improves sperm mobility and preservation of membrane integrity upon thawing (*60*, *61*). This study reveals that in *C. elegans*, proline catabolism impacts several functional qualities of sperm. Loss of proline catabolism results in smaller sperm with impaired activation, two qualities that directly impact competitive advantage. As such, proline biosynthesis, catabolism, and steady state concentrations must be tightly regulated, and the importance of proline in cellular homeostasis may help explain the transcriptional responses measured in animals with dysfunctional *alh-6* (**Figures 3 and 4**).

Our previous work defined the age-dependent decline in function of somatic tissues, particularly muscle in animals lacking functional ALH-6 (35, 36), which is not manifested until Day 3 of adulthood. This study reveals that although somatic phenotypes are observed post-developmentally, the germline and specifically sperm are sensitive to loss of *alh-6* much earlier in development (phenotypes assayed at L4 or Day 1 of adulthood), with many physiological consequences from dysregulation of metabolism. Reproductive senescence is a field of growing significance as the number of couples that choose to delay having children increases. About 30-40% of all male infertility cases are associated with increased levels of ROS, yet we don't understand the underlying mechanism (76). Additionally, sperm quality has been shown to decline with age, as ROS content increases with age (7, 8, 77, 78), demonstrating the link between ROS and male reproductive senescence. Our study demonstrates that perturbation of mitochondrial proline catabolism, particularly mutation in *alh-6/ALDH4A1*, leads to redox imbalance and impaired sperm function. Importantly, addition of antioxidants to diet can abrogate this sperm dysfunction (**Figures 5D-E**), implicating the potential therapeutic effects of antioxidant supplement in male infertility arising from redox imbalance.

Recent studies have focused on the role of NAD+ metabolism in cellular health, while the impact of FAD has received less attention. FAD levels are diminished in *alh-6* animals specifically at the L4 stage when spermatogenesis is occurring (**Figure 4B**). Riboflavin (Vitamin $B_2$) is a precursor to FAD and flavin

mononucleotide (FMN) cofactors that are needed for metabolic reactions (like proline catabolism and mitochondrial oxidative phosphorylation) to maintain proper cellular function. Despite its importance, humans lack a riboflavin biosynthetic pathway and therefore require riboflavin from exogenous sources (79). Insufficient intake can lead to impairment of flavin homeostasis, which is associated with cancer, cardiovascular diseases, anemia, neurological disorders, fetal development, etc. (79). Our study suggests that riboflavin and FAD play critical roles in reproduction as *alh-6* mutants suffer from sperm dysfunction driven by a reduction in FAD levels (**Figure 4**). Importantly, these sperm specific defects can be corrected by dietary supplementation of vitamin $B_2$, which in light of the exceptional conservation of mitochondrial homeostatic pathways, suggest the nutraceutical role vitamin $B_2$ could play in sperm health across species.

Our study also demonstrates that spermatids lacking *alh-6* have increased mitochondrial fusion; a perturbation at the mitochondrial organelle structure-level that contributes to the sperm-specific phenotypes observed. In addition to prior work showing *fzo-1/MFN1/MFN2* and *drp-1*/*DRP-1* to be important for mitochondrial elimination post-fertilization (69), our work reveals that mitochondrial fission and fusion machinery are present and active in spermatids and that perturbation of these dynamics can affect sperm maturation and competitive fitness (**Figure 6**). Future work to define how *alh-6* spermatids use mitophagy, which can clear damaged mitochondria, will be of interest. In conclusion, our work identifies proline metabolism as a major metabolic pathway that can impact sperm maturation and male reproductive success. Moreover, these studies identify specific interventions to reverse the redox imbalance, cofactor depletion, and altered mitochondria dynamics, all of which play a part in sperm dysfunction resulting from proline metabolism defects.

## ACKNOWLEDGEMENTS

We thank K. Han and L. Thomas for technical assistance, and H. Dalton and A. Hammerquist for critical reading of the manuscript. Some strains were provided by the CGC, which is funded by the NIH Office of Research Infrastructure Programs (P40 OD010440). This work was funded by the NIH (GM109028) and the Ellison Medical Foundation (S.P.C.) and the American Federation of Aging Research (C-A.Y. and S.P.C).

## AUTHOR CONTRIBUTIONS

S.P.C. designed the study; C-A.Y., D.L.R., N.M., S.P., and S.P.C. performed the experiments; C-A.Y. and S.P.C. analyzed data and wrote the manuscript. All authors discussed the results and commented on the manuscript.

## COMPETING INTERESTS

The authors declare no competing interests.

## DATA AVAILABILITY

All relevant data are available from the authors.

## METHODS

### *C. elegans* strains and maintenance

*C. elegans* were cultured using standard techniques at 20°C. The following strains were used: wild type (WT) N2 Bristol, CB4856 (HW), SPC321[*alh-6(lax105)*], SP326[*alh-6p;alh-6::gfp*], CL2166[*gst4-p::gfp*], SPC223[*alh-6(lax105);gst-4p::gfp*], and CU6372[*drp-1(tm1108)*]. Double and triple mutants were generated by standard genetic techniques. *E. coli* strains used were as follows: B Strain OP50(80) and HT115(DE3) [F$^-$mcrA mcrB IN(rrnD-rrnE)1 lambda$^-$ rnc14::Tn10 λ(DE3)](81). For dietary supplement assays, the following were added to the NGM plate mix to final concentration: 5mM NAC, 2.5mM riboflavin. RNAi experiments done using OP50 RNAi *E. coli* B strain as described in (82) yielded similar results as HT115-based RNAi. All strains were adapted to diets for at least three generations and strains were never allowed to starve.

### EMS mutagenesis

Ethyl methanesulfonate (EMS) mutagenesis was performed as previously described (57). Briefly, SPC223[*alh-6(lax105);gst-4p::gfp*] was mutagenized with EMS, and F2 worms with reduced GFP expression (indicating suppression of SKN-1 activation) were selected. *prdh-1(lax228)* was isolated and mapped to chromosome IV. Whole genome sequencing and injection rescue confirmed mutant sequence identity.

### Microscopy

Zeiss Axio Imager and ZEN software were used to acquire all images used in this study. For GFP reporter strains, worms were mounted in M9 with 10mM levamisole and imaged with DIC and GFP filters. For sperm number assay samples were imaged with DIC and DAPI filters in z-stacks. For sperm size and activation assays, dissected sperm samples were mounted with coverslip and imaged at 100x with DIC filter on two different focal planes for each field to ensure accuracy. For sperm mitochondria assays, dissected sperm samples were covered with coverslip and imaged at 100x with DIC, GFP, and RFP filters in z-stacks to assess overall mitochondria content within each spermatid.

### Fertility assay

Worms were egg prepped and eggs were allowed to hatch overnight. The next day synchronized L1 larvae were dropped on NGM plates seeded with either OP50 or HT115. 48 hrs later, at least ten L4 hermaphrodites for each genotype were singled onto individual plates and moved every 14 hours until egg laying ceased. Progeny were counted 48 hours after the singled hermaphrodite was moved to a different place. Plates were counted twice for accuracy.

### Mated reproductive assay

Males were synchronized by egg laying, picked as L4 larvae for use as young adults for mating experiments. L4 hermaphrodites were each put on a plate with 30ul of OP50 seeded in the center together with three young adult males. 24hrs post mating, males are removed, and each hermaphrodite was moved to a new plate every 24 hr until egg laying ceases. Progeny were counted 48 hours after hermaphrodite was moved from the plate. For sperm competition assay progeny with GFP fluorescence were counted from the cohort. Plates were counted twice for accuracy.

### Cofactor Measurements

Worms were egg prepped and eggs were allowed to hatch overnight. Next day, synchronized L1s were dropped on NGM plates seeded with concentrated OP50. FAD levels are measured following directions in FAD Colorimetric/Fluorometric Assay Kit (K357) from BioVision.

### Sperm Number Assay

Worms were egg prepped and eggs were allowed to hatch overnight. Next day, synchronized L1s were dropped on seeded NGM plates. 72 hrs post drop, day 1 adult animals were washed 3x with 1xPBST, fixed with 40% 2-propanol, and stained with DAPI for 2 hrs. Samples were washed for 30min with PBST, mounted with vectashield mounting medium, and covered with coverslip to image.

**Sperm Size Assay**

Males were isolated at L4 stage 24 hour before assay. For each strain, five day 1 adult males were dissected in 35μL pH 7.8 SM buffer (50mM HEPES, 50mM NaCl, 25mM KCl, 5mM $CaCl_2$, 1mM $MgSO_4$, 10mM dextrose) with DAPI to release spermatids and imaged.

**Sperm Activation with Pronase**

Males were isolated at L4 stage 24 hour before assay. For each strain, five day 1 adult males were dissected in 35μL pH 7.8 SM buffer (50mM HEPES, 50mM NaCl, 25mM KCl, 5mM $CaCl_2$, 1mM $MgSO_4$, 1mg/ml BSA) supplemented with 200μg/mL Pronase to release spermatids. Another 25ul of same solution was added and the spermatids were incubated at RT for 30 min for activation to occur.

**Sperm Mitochondria Staining**

Males were isolated at L4 stage 24 hour before assay. For each strain, five day 1 adult males were dissected in 35μL pH 7.8 SM buffer (50mM HEPES, 50mM NaCl, 25mM KCl, 5mM $CaCl_2$, 1mM $MgSO_4$, 1mg/ml BSA) with JC-1(Thermo Fisher Scientific T3168) added to 10μM final concentration. Another 25ul of same solution is added and the spermatids are incubated at RT for 10 min. Then the slide was washed three times with 100ul SM buffer before imaging.

**RNA-sequencing**

Worms were egg prepped and eggs were allowed to hatch overnight. Next day, synchronized L1s were dropped on NGM plates seeded with concentrated OP50. 48 and 120 hrs post drop, L4 animals and day 3 adult animals, respectively, were washed 3 times with M9 and frozen in TRI Reagent at -80°C. Animals are homogenized and RNA extraction is performed following protocol in Zymo Direct-zol RNA Isolation Kit. RNA samples were sequenced and analyzed by Novogene.

**Statistical analysis**

Data are presented as mean ± SEM. Comparisons and significance were analyzed in Graphpad Prism 7. Comparisons between two groups were done using Student's Test. Comparisons between more than two groups were done using ANOVA. For sperm activation assays, Fisher's Exact Test was used and p-values are adjusted for multiple comparisons. *p<0.05 **p<0.01 *** p<0.001 ****<0.0001

## REFERENCES


1. Mills M, *et al.* (2011) Why do people postpone parenthood? Reasons and social policy incentives. *Hum Reprod Update* 17(6):848-860.
2. Lemaitre JF & Gaillard JM (2017) Reproductive senescence: new perspectives in the wild. *Biol Rev Camb Philos Soc* 92(4):2182-2199.
3. Baird DT, *et al.* (2005) Fertility and ageing. *Hum Reprod Update* 11(3):261-276.
4. Treloar AE (1981) Menstrual cyclicity and the pre-menopause. *Maturitas* 3(3-4):249-264.
5. Kadandale P & Singson A (2004) Oocyte production and sperm utilization patterns in semi-fertile strains of Caenorhabditis elegans. *BMC Dev Biol* 4:3.
6. Luo S, Kleemann GA, Ashraf JM, Shaw WM, & Murphy CT (2010) TGF-beta and insulin signaling regulate reproductive aging via oocyte and germline quality maintenance. *Cell* 143(2):299-312.
7. Cocuzza M, *et al.* (2008) Age-related increase of reactive oxygen species in neat semen in healthy fertile men. *Urology* 71(3):490-494.
8. Kidd SA, Eskenazi B, & Wyrobek AJ (2001) Effects of male age on semen quality and fertility: a review of the literature. *Fertil Steril* 75(2):237-248.
9. Ozkosem B, Feinstein SI, Fisher AB, & O'Flaherty C (2015) Advancing age increases sperm chromatin damage and impairs fertility in peroxiredoxin 6 null mice. *Redox Biol* 5:15-23.
10. Sena LA & Chandel NS (2012) Physiological roles of mitochondrial reactive oxygen species. *Mol Cell* 48(2):158-167.
11. Murphy MP (2009) How mitochondria produce reactive oxygen species. *Biochem J* 417(1):1-13.
12. Mundy AJ, Ryder TA, & Edmonds DK (1995) Asthenozoospermia and the human sperm mid-piece. *Hum Reprod* 10(1):116-119.
13. Pelliccione F, *et al.* (2011) Altered ultrastructure of mitochondrial membranes is strongly associated with unexplained asthenozoospermia. *Fertil Steril* 95(2):641-646.
14. Ruiz-Pesini E, *et al.* (2000) Human mtDNA haplogroups associated with high or reduced spermatozoa motility. *Am J Hum Genet* 67(3):682-696.
15. Diez-Sanchez C, *et al.* (2003) Mitochondrial DNA content of human spermatozoa. *Biol Reprod* 68(1):180-185.
16. Nakada K, *et al.* (2006) Mitochondria-related male infertility. *Proc Natl Acad Sci U S A* 103(41):15148-15153.
17. Amaral A, Ramalho-Santos J, & St John JC (2007) The expression of polymerase gamma and mitochondrial transcription factor A and the regulation of mitochondrial DNA content in mature human sperm. *Hum Reprod* 22(6):1585-1596.
18. Song GJ & Lewis V (2008) Mitochondrial DNA integrity and copy number in sperm from infertile men. *Fertil Steril* 90(6):2238-2244.
19. Zhao C, *et al.* (2007) Identification of several proteins involved in regulation of sperm motility by proteomic analysis. *Fertil Steril* 87(2):436-438.
20. Martinez-Heredia J, de Mateo S, Vidal-Taboada JM, Ballesca JL, & Oliva R (2008) Identification of proteomic differences in asthenozoospermic sperm samples. *Hum Reprod* 23(4):783-791.
21. Chan CC, *et al.* (2009) Motility and protein phosphorylation in healthy and asthenozoospermic sperm. *J Proteome Res* 8(11):5382-5386.
22. Ruiz-Pesini E, *et al.* (1998) Correlation of sperm motility with mitochondrial enzymatic activities. *Clin Chem* 44(8 Pt 1):1616-1620.
23. Ruiz-Pesini E, *et al.* (2000) Seminal quality correlates with mitochondrial functionality. *Clin Chim Acta* 300(1-2):97-105.
24. Narisawa S, *et al.* (2002) Testis-specific cytochrome c-null mice produce functional sperm but undergo early testicular atrophy. *Mol Cell Biol* 22(15):5554-5562.
25. de Lamirande E & Gagnon C (1993) A positive role for the superoxide anion in triggering hyperactivation and capacitation of human spermatozoa. *Int J Androl* 16(1):21-25.

26. Kodama H, Kuribayashi Y, & Gagnon C (1996) Effect of sperm lipid peroxidation on fertilization. *J Androl* 17(2):151-157.
27. Leclerc P, de Lamirande E, & Gagnon C (1997) Regulation of protein-tyrosine phosphorylation and human sperm capacitation by reactive oxygen derivatives. *Free Radic Biol Med* 22(4):643-656.
28. Tremellen K (2008) Oxidative stress and male infertility--a clinical perspective. *Hum Reprod Update* 14(3):243-258.
29. Agarwal A, Virk G, Ong C, & du Plessis SS (2014) Effect of oxidative stress on male reproduction. *World J Mens Health* 32(1):1-17.
30. Koppers AJ, De Iuliis GN, Finnie JM, McLaughlin EA, & Aitken RJ (2008) Significance of mitochondrial reactive oxygen species in the generation of oxidative stress in spermatozoa. *J Clin Endocrinol Metab* 93(8):3199-3207.
31. Aitken RJ*, et al.* (2012) Sperm motility is lost in vitro as a consequence of mitochondrial free radical production and the generation of electrophilic aldehydes but can be significantly rescued by the presence of nucleophilic thiols. *Biol Reprod* 87(5):110.
32. Grad LI & Lemire BD (2004) Mitochondrial complex I mutations in Caenorhabditis elegans produce cytochrome c oxidase deficiency, oxidative stress and vitamin-responsive lactic acidosis. *Hum Mol Genet* 13(3):303-314.
33. Jonassen T, Marbois BN, Faull KF, Clarke CF, & Larsen PL (2002) Development and fertility in Caenorhabditis elegans clk-1 mutants depend upon transport of dietary coenzyme Q8 to mitochondria. *J Biol Chem* 277(47):45020-45027.
34. Adams E & Frank L (1980) Metabolism of proline and the hydroxyprolines. *Annu Rev Biochem* 49:1005-1061.
35. Pang S & Curran SP (2014) Adaptive Capacity to Bacterial Diet Modulates Aging in C. elegans. *Cell Metab* 19(2):221-231.
36. Pang S, Lynn DA, Lo JY, Paek J, & Curran SP (2014) SKN-1 and Nrf2 couples proline catabolism with lipid metabolism during nutrient deprivation. *Nat Commun* 5:5048.
37. Deuschle K*, et al.* (2004) The role of [Delta]1-pyrroline-5-carboxylate dehydrogenase in proline degradation. *Plant Cell* 16(12):3413-3425.
38. Miller G*, et al.* (2009) Unraveling delta1-pyrroline-5-carboxylate-proline cycle in plants by uncoupled expression of proline oxidation enzymes. *J Biol Chem* 284(39):26482-26492.
39. Nomura M & Takagi H (2004) Role of the yeast acetyltransferase Mpr1 in oxidative stress: regulation of oxygen reactive species caused by a toxic proline catabolism intermediate. *Proc Natl Acad Sci U S A* 101(34):12616-12621.
40. Palikaras K, Lionaki E, & Tavernarakis N (2015) Coupling mitogenesis and mitophagy for longevity. *Autophagy* 11(8):1428-1430.
41. Liau WS, Gonzalez-Serricchio AS, Deshommes C, Chin K, & LaMunyon CW (2007) A persistent mitochondrial deletion reduces fitness and sperm performance in heteroplasmic populations of C. elegans. *BMC Genet* 8:8.
42. Amaral A, Lourenco B, Marques M, & Ramalho-Santos J (2013) Mitochondria functionality and sperm quality. *Reproduction* 146(5):R163-174.
43. Ramalho-Santos J & Amaral S (2013) Mitochondria and mammalian reproduction. *Mol Cell Endocrinol* 379(1-2):74-84.
44. McCarter J, Bartlett B, Dang T, & Schedl T (1999) On the control of oocyte meiotic maturation and ovulation in Caenorhabditis elegans. *Dev Biol* 205(1):111-128.
45. Ward S & Miwa J (1978) Characterization of temperature-sensitive, fertilization-defective mutants of the nematode caenorhabditis elegans. *Genetics* 88(2):285-303.
46. Argon Y & Ward S (1980) Caenorhabditis elegans fertilization-defective mutants with abnormal sperm. *Genetics* 96(2):413-433.
47. Ward S & Carrel JS (1979) Fertilization and sperm competition in the nematode Caenorhabditis elegans. *Dev Biol* 73(2):304-321.

48. LaMunyon CW & Ward S (1995) Sperm precedence in a hermaphroditic nematode (Caenorhabditis elegans) is due to competitive superiority of male sperm. *Experientia* 51(8):817-823.
49. Singson A, Hill KL, & L'Hernault SW (1999) Sperm competition in the absence of fertilization in Caenorhabditis elegans. *Genetics* 152(1):201-208.
50. Hirsh D, Oppenheim D, & Klass M (1976) Development of the reproductive system of Caenorhabditis elegans. *Dev Biol* 49(1):200-219.
51. Hansen JM, Chavez DR, & Stanfield GM (2015) COMP-1 promotes competitive advantage of nematode sperm. *Elife* 4.
52. LaMunyon CW & Ward S (2002) Evolution of larger sperm in response to experimentally increased sperm competition in Caenorhabditis elegans. *Proc Biol Sci* 269(1496):1125-1128.
53. LaMunyon CW & Ward S (1998) Larger sperm outcompete smaller sperm in the nematode Caenorhabditis elegans. *Proc Biol Sci* 265(1409):1997-2002.
54. Ward S, Hogan E, & Nelson GA (1983) The initiation of spermiogenesis in the nematode Caenorhabditis elegans. *Dev Biol* 98(1):70-79.
55. Shakes DC & Ward S (1989) Initiation of spermiogenesis in C. elegans: a pharmacological and genetic analysis. *Dev Biol* 134(1):189-200.
56. Blackwell TK, Steinbaugh MJ, Hourihan JM, Ewald CY, & Isik M (2015) SKN-1/Nrf, stress responses, and aging in Caenorhabditis elegans. *Free Radic Biol Med* 88(Pt B):290-301.
57. Paek J*, et al.* (2012) Mitochondrial SKN-1/Nrf mediates a conserved starvation response. *Cell Metab* 16(4):526-537.
58. Glover-Cutter KM, Lin S, & Blackwell TK (2013) Integration of the unfolded protein and oxidative stress responses through SKN-1/Nrf. *PLoS Genet* 9(9):e1003701.
59. An JH & Blackwell TK (2003) SKN-1 links C. elegans mesendodermal specification to a conserved oxidative stress response. *Genes & development* 17(15):1882-1893.
60. Lynn DA*, et al.* (2015) Omega-3 and -6 fatty acids allocate somatic and germline lipids to ensure fitness during nutrient and oxidative stress in Caenorhabditis elegans. *Proc Natl Acad Sci U S A* 112(50):15378-15383.
61. Palikaras K, Lionaki E, & Tavernarakis N (2015) Coordination of mitophagy and mitochondrial biogenesis during ageing in C. elegans. *Nature* 521(7553):525-528.
62. Burch HB, Combs AM, Lowry OH, & Padilla AM (1956) Effects of riboflavin deficiency and realimentation on flavin enzymes of tissues. *J Biol Chem* 223(1):29-45.
63. Redondo A, Menasche P, & Le Beau J (1975) [Operation for stenosis of the internal carotid artery secondary to irradiation (a propos of 1 observation)]. *Neurochirurgie* 21(3):239-245.
64. Blankenberg D*, et al.* (2010) Galaxy: a web-based genome analysis tool for experimentalists. *Curr Protoc Mol Biol* Chapter 19:Unit 19 10 11-21.
65. Yoon KA, Nakamura Y, & Arakawa H (2004) Identification of ALDH4 as a p53-inducible gene and its protective role in cellular stresses. *J Hum Genet* 49(3):134-140.
66. Tondera D*, et al.* (2009) SLP-2 is required for stress-induced mitochondrial hyperfusion. *Embo J* 28(11):1589-1600.
67. Gomes LC, Di Benedetto G, & Scorrano L (2011) Essential amino acids and glutamine regulate induction of mitochondrial elongation during autophagy. *Cell Cycle* 10(16):2635-2639.
68. Rambold AS, Kostelecky B, Elia N, & Lippincott-Schwartz J (2011) Tubular network formation protects mitochondria from autophagosomal degradation during nutrient starvation. *Proc Natl Acad Sci U S A* 108(25):10190-10195.
69. Wang Y*, et al.* (2016) Kinetics and specificity of paternal mitochondrial elimination in Caenorhabditis elegans. *Nat Commun* 7:12569.
70. Smirnova E, Griparic L, Shurland DL, & van der Bliek AM (2001) Dynamin-related protein Drp1 is required for mitochondrial division in mammalian cells. *Mol Biol Cell* 12(8):2245-2256.
71. Lima AR*, et al.* (2018) Dynamin-Related Protein 1 at the Crossroads of Cancer. *Genes (Basel)* 9(2).

72. van der Bliek AM, Sedensky MM, & Morgan PG (2017) Cell Biology of the Mitochondrion. *Genetics* 207(3):843-871.
73. Shaw JM & Nunnari J (2002) Mitochondrial dynamics and division in budding yeast. *Trends Cell Biol* 12(4):178-184.
74. Wagner H, Cheng JW, & Ko EY (2018) Role of reactive oxygen species in male infertility: An updated review of literature. *Arab J Urol* 16(1):35-43.
75. Cocuzza M, Sikka SC, Athayde KS, & Agarwal A (2007) Clinical relevance of oxidative stress and sperm chromatin damage in male infertility: an evidence based analysis. *Int Braz J Urol* 33(5):603-621.
76. Jose-Miller AB, Boyden JW, & Frey KA (2007) Infertility. *Am Fam Physician* 75(6):849-856.
77. Jung A, Schuppe HC, & Schill WB (2002) Comparison of semen quality in older and younger men attending an andrology clinic. *Andrologia* 34(2):116-122.
78. Plastira K*, et al.* (2007) The effects of age on DNA fragmentation, chromatin packaging and conventional semen parameters in spermatozoa of oligoasthenoteratozoospermic patients. *J Assist Reprod Genet* 24(10):437-443.
79. Powers HJ (2003) Riboflavin (vitamin B-2) and health. *Am J Clin Nutr* 77(6):1352-1360.
80. Brenner S (1974) The genetics of Caenorhabditis elegans. *Genetics* 77(1):71-94.
81. Timmons L, Court DL, & Fire A (2001) Ingestion of bacterially expressed dsRNAs can produce specific and potent genetic interference in Caenorhabditis elegans. *Gene* 263(1-2):103-112.
82. Dalton HM & Curran SP (2018) Hypodermal responses to protein synthesis inhibition induce systemic developmental arrest and AMPK-dependent survival in Caenorhabditis elegans. *PLoS Genet* 14(7):e1007520.

## FIGURES

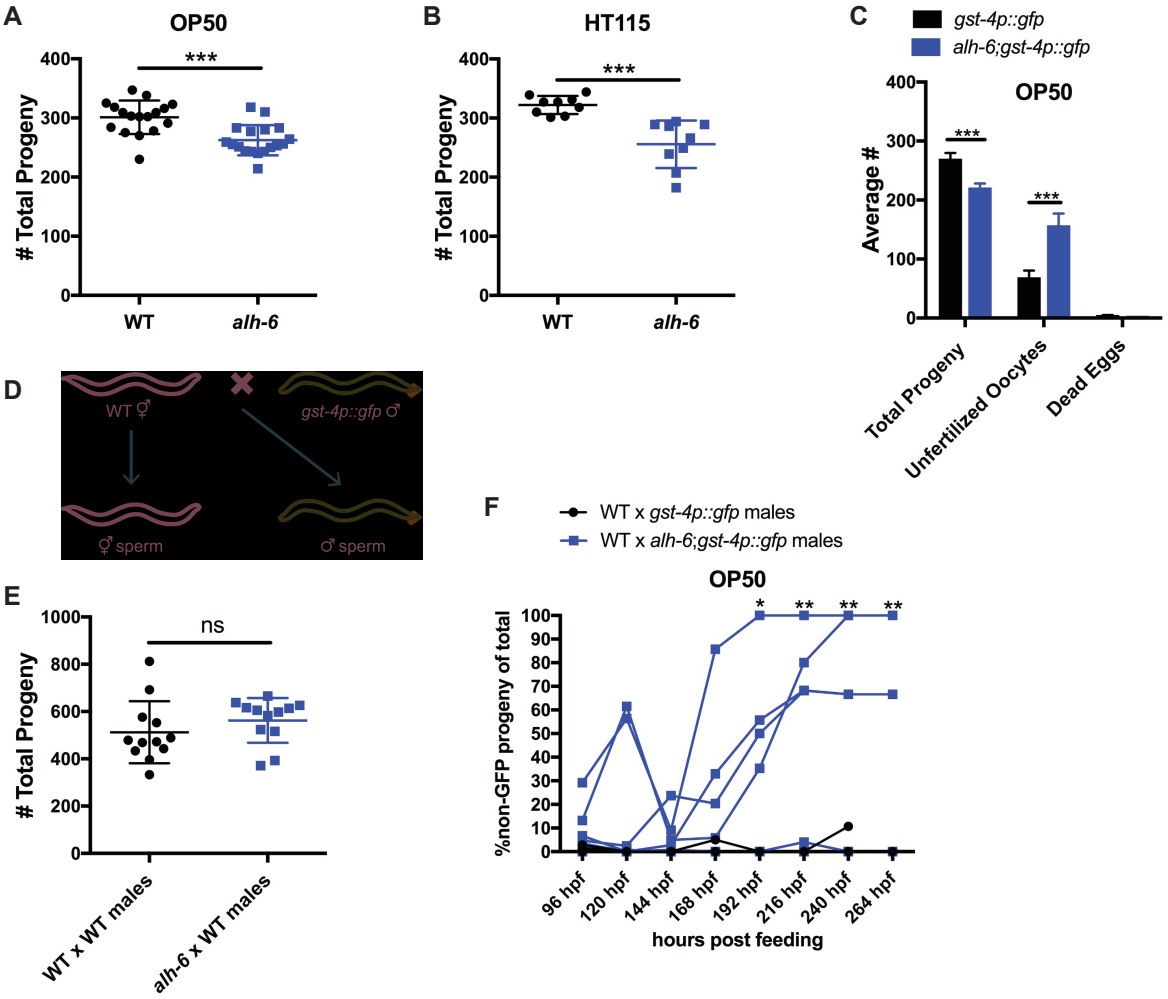


**Figure 1. *alh-6* fertility defects are sperm-specific.** (a-b) *alh-6* hermaphrodites have reduced brood size when fed OP50 (a) or HT115 (b) diets. (c) *alh-6* hermaphrodites have increased unfertilized oocytes and few dead embryos. (d) Mated reproductive assay scheme utilizes males to maximize reproductive output (as in e) and can exploit males harboring GFP to differentiate progeny resulting from self- versus male-sperm (as in f). (e) Wild type (WT) and *alh-6* hermaphrodites mated with WT males yield similar number of total progeny. (f) WT hermaphrodites mated with *alh-6;gst-4p::gfp* yield more non-GFP progeny, indicating self-fertilization, than hermaphrodites mated with wild type males harboring *gst-4p::gfp*. Statistical comparisons by unpaired t-test. *, p<0.05; **, p<0.01; ***, p<0.001; ****, p<0.0001. All studies performed in biological triplicate; refer to Table S1 for n for each comparison.

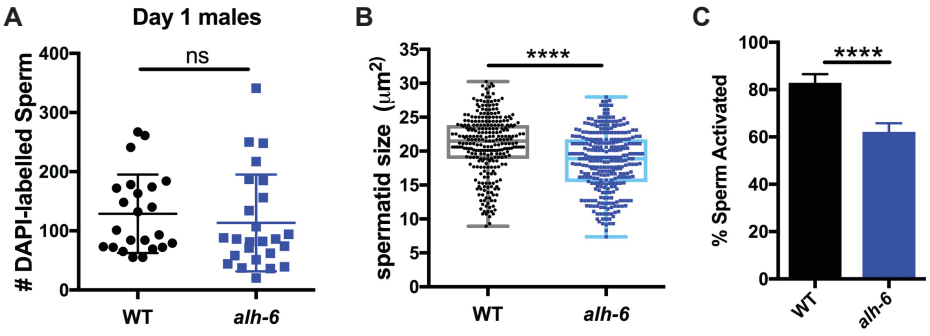


**Figure 2. *alh-6* males have sperm defects.** (a) Sperm quantity is similar between wild type (WT) and *alh-6* mutant day 1 adult males. (b) Spermatid size is reduced in *alh-6* mutant day 1 adult males as compared to age matched WT males. (c) Sperm activation is impaired in *alh-6* mutant day 1 adult males relative to age-matched WT males. Statistical comparisons of sperm number and size by unpaired t-test and sperm activation by Fisher's exact test. *, $p<0.05$; **, $p<0.01$; ***, $p<0.001$; ****, $p<0.0001$. All studies performed in biological triplicate; refer to Table S1 for n for each comparison.

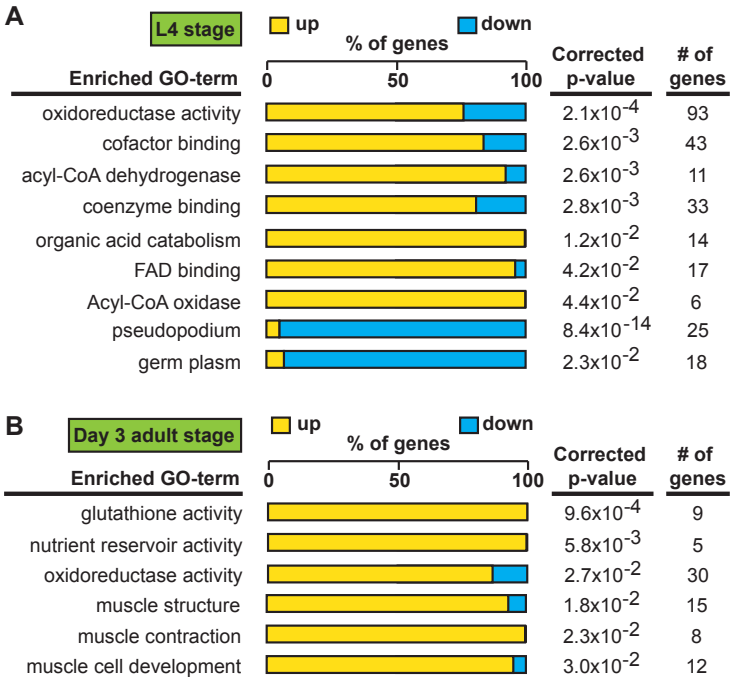


**Figure 3. Transcriptional patterns define developmental- and adult-specific consequences to loss of *alh-6* activity.** Gene Ontology (GO) term enrichment analysis of RNAseq data. (a) Transcriptional changes at L4 stage are enriched for metabolism and sperm-specific genes. (b) Transcriptional changes at day 3 adulthood are enriched for changes in glutathione activity, oxidoreductase activity, and muscle-specific genes.

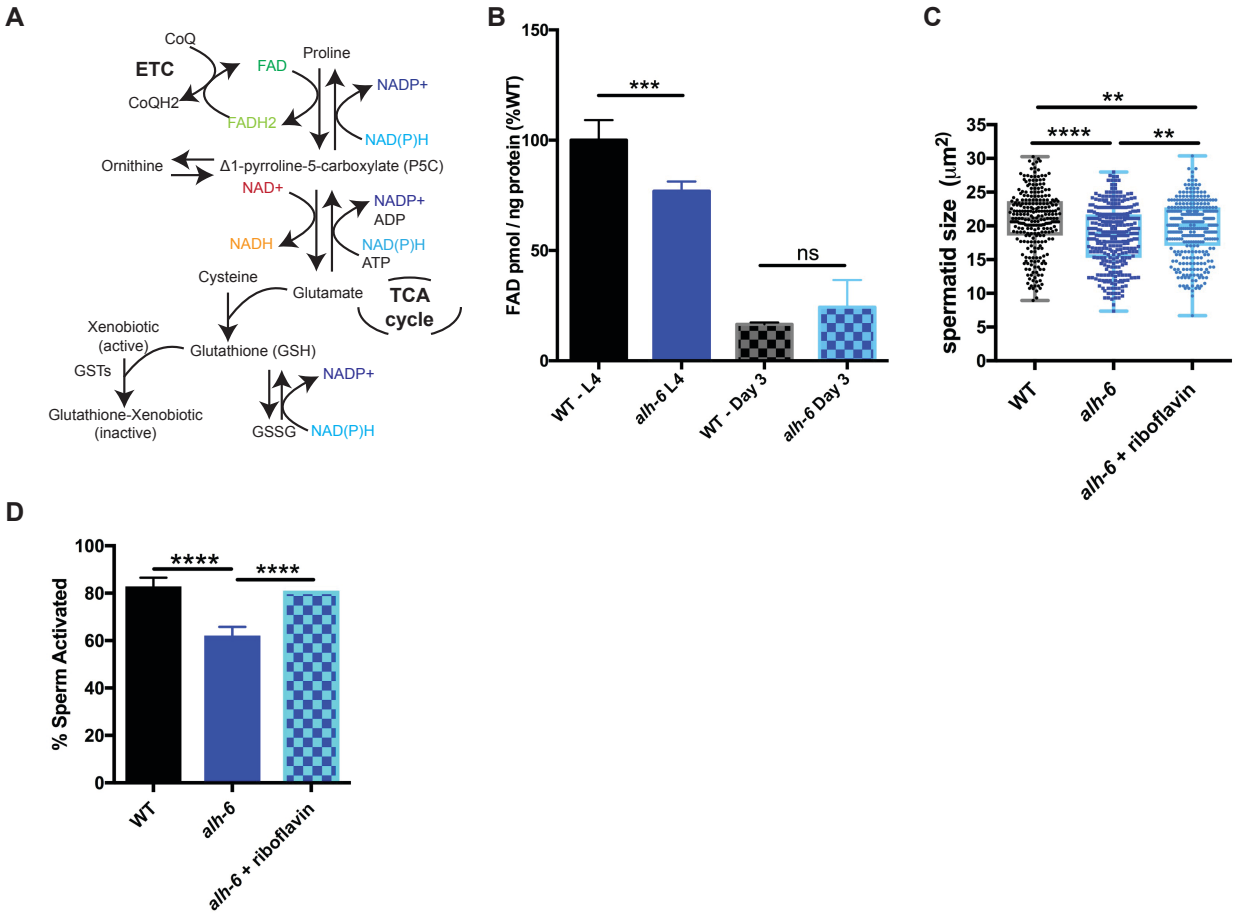


**Figure 4. Loss of FAD homeostasis in *alh-6* mutants leads to sperm dysfunction.** (a) Metabolic pathways utilize adenine dinucleotide cofactors to maintain redox balance in cells. (b) FAD+ levels are reduced in *alh-6* mutant animals at the L4 developmental stage. (c-d) Dietary supplement of riboflavin restores sperm size (c) and sperm activation (d) in sperm from *alh-6* mutants. Statistical comparisons of sperm size by ANOVA. Statistical comparisons of activation by fisher's exact test with p-value cut-off adjusted by number of comparisons. *, $p<0.05$; **, $p<0.01$; ***, $p<0.001$; ****, $p<0.0001$. All studies performed in biological triplicate; refer to Table S1 for n for each comparison.

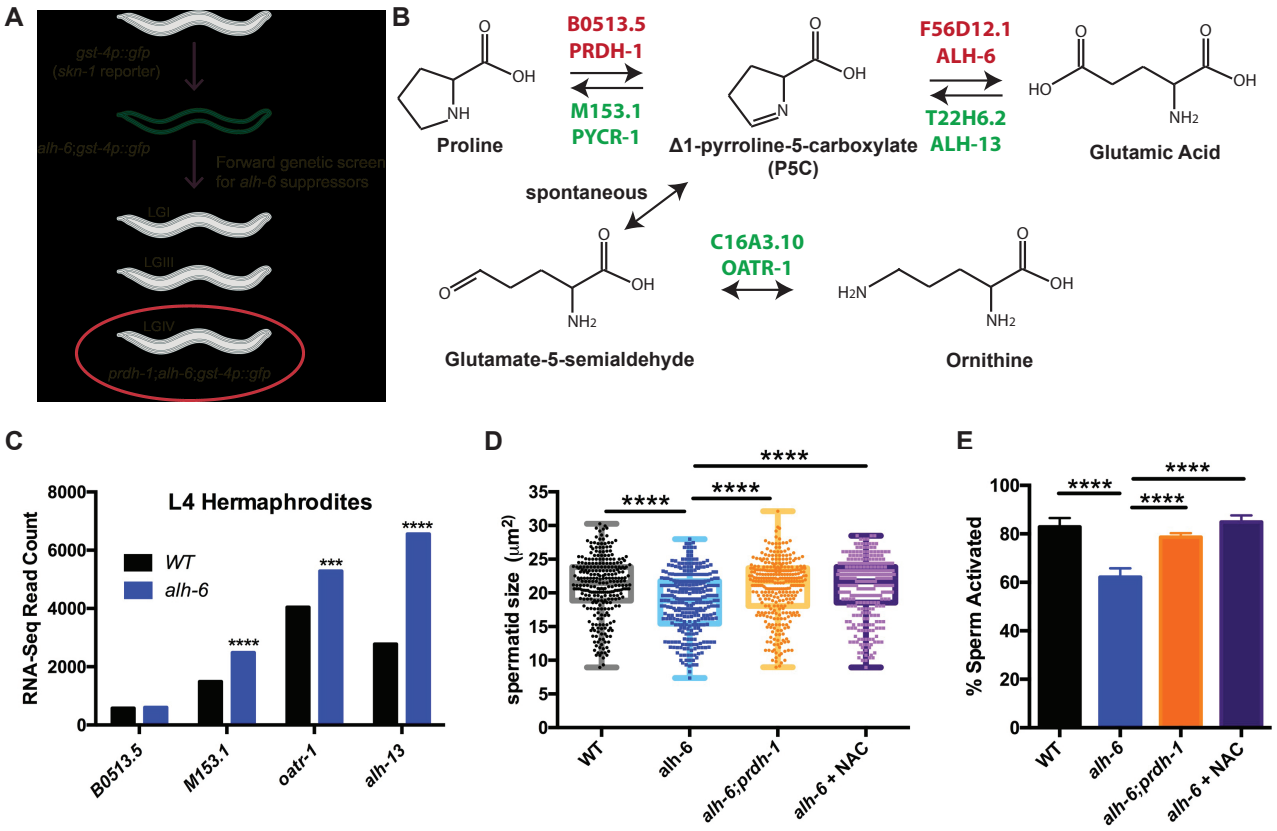


**Figure 5. Redox imbalance drives sperm defects in *alh-6* mutants.** (a) Cartoon depiction of EMS screen for suppressors of the SKN-1 reporter activation in *alh-6* mutants. (b) Schematic of biosynthetic and catabolic pathways of proline in *C. elegans*. (c) *M153.1*, *oatr-1*, and *alh-13* are upregulated in *alh-6* mutant L4 animals. (d-e) *prdh-1* mutation or dietary antioxidant supplementation rescues sperm size (d) and spermatid activation (e). Statistical comparisons of sperm size by ANOVA and statistical comparisons of sperm activation by Fisher's exact test with p-value cut-off adjusted by number of comparisons. *, p<0.05; **, p<0.01; ***, p<0.001; ****, p<0.0001. All studies performed in biological triplicate; refer to Table S1 for n for each comparison.

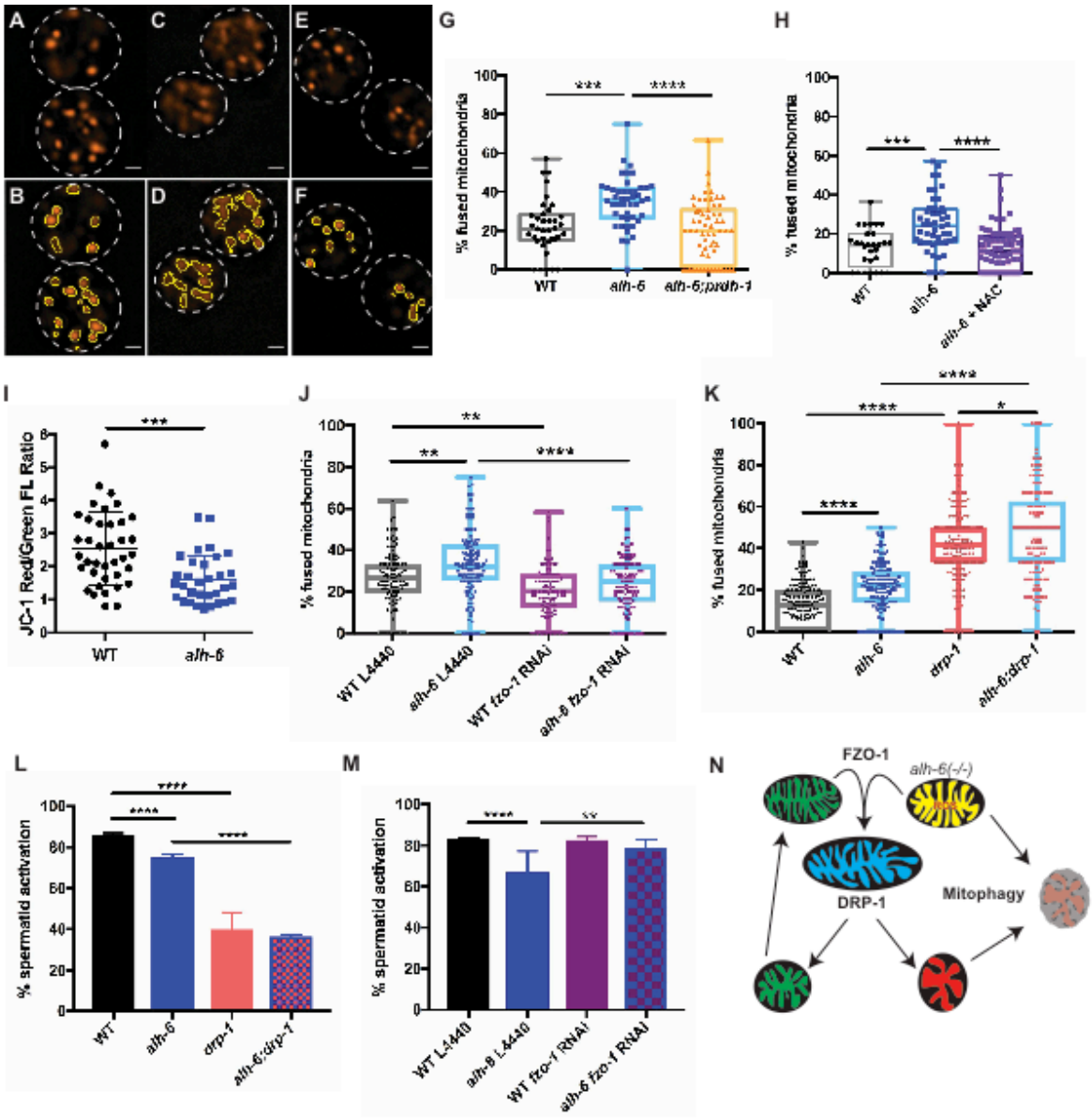


**Figure 6. Mitochondrial dynamics drive sperm quality. (a-f)** JC-1 dye stained mitochondria of WT (a-b), *alh-6* mutant (c-d), *prdh-1;alh-6* mutant (e-f) spermatids from dissected males; b, d, f are ImageJ detection of JC-1 stained sperm mitochondria area. (g) *alh-6* mutant male spermatids have increased number of fused mitochondria, which is restored to WT levels in *prdh-1;alh-6* mutants. (h) Antioxidant treatment restores mitochondrial dynamics to wild type levels in *alh-6* mutant spermatids. (i) Mitochondria in *alh-6* mutant spermatids have reduced JC-1 red/green fluorescence ratio, indicating mitochondria depolarization. (j) *fzo-1* RNAi decreases mitochondrial fusion in both WT and *alh-6* mutant spermatids. (k) *drp-1* mutation increases mitochondrial fusion in spermatids. (l) *drp-1* mutation significantly impairs sperm activation in both WT and *alh-6* mutant spermatids. (m) *fzo-1* RNAi restores sperm activation in *alh-6* mutant (n) Model: *alh-6* mutation results in increased fusion in sperm mitochondria that is mediated by *fzo*-1, which results in impaired sperm activation. Statistical comparisons of JC-1 Red/Green FL ratio by unpaired t-test. Statistical comparisons of mitochondria fusion by ANOVA. Statistical comparisons of sperm activation by Fisher's exact test with p-value cut-off adjusted by number of comparisons. *, $p<0.05$; **, $p<0.01$; ***, $p<0.001$; ****, $p<0.0001$. All studies performed in biological triplicate; refer to Table S1 for n for each comparison.

## SUPPLEMENTAL FIGURE LEGENDS

**Figure S1. Cartoon depiction of proline catabolism pathway in *C. elegans*.**

**Figure S2. ALH-6 expression in the germline.** UV integrated *alh-6::gfp* strain under its endogenous promoter reveal expression of ALH-6 in hermaphrodite (a-b) and male (c-d) germline. a and c are DIC images while b and b are GFP images.

**Figure S3. *alh-6* hermaphrodite reproductive span is similar to wild type (WT) on different diets.** Progeny output time-courses are plotted as % total progeny for each time point. WT and *alh-6* mutant have similar output on OP50 (a) and HT115 (b). Significance indicate differences in progeny output at a particular time point done by multiple t-tests. *, p<0.05; **, p<0.01; ***, p<0.001; ****, p<0.0001. All studies performed in biological triplicate; refer to Table S1 for n for each comparison.

**Figure S4. *alh-6* fertility defects are sperm-specific.** (a) Day 4 adult WT hermaphrodites mated to either *gst-4p::gfp* or *alh-6;gst-4p::gfp* males yield similar total brood size. (b) Day 4 adult *alh-6* hermaphrodites mated to either *gst-4p::gfp* or *alh-6;gst-4p::gfp* males yield similar total brood size. Comparisons made with unpaired t-test. *, p<0.05; **, p<0.01; ***, p<0.001; ****, p<0.0001. All studies performed in biological triplicate; refer to Table S1 for n for each comparison.

**Figure S5. Sperm defects in *alh-6* mutants.** (a) *alh-6* hermaphrodites have reduced sperm number as day 1 adults. (b) Spermiogenesis stages. Spermatozoa with fully formed pseudopods are considered activated.

**Figure S6. RNA-Sequencing data of WT and *alh-6* hermaphrodites at L4 and day 3 adulthood.** (a) Number of genes that are significantly upregulated in *alh-6(lax105)* compared to WT at L4 and Day 3 adult stages. (b) Number of genes that are significantly downregulated in *alh-6(lax105)* compared to WT at L4 and Day 3 adult stages. FDR = 0.05. All studies performed in biological triplicate; refer to Table S1 for n for each comparison.

**Figure S7. Adenine nucleotide cofactor homeostasis is disrupted in *alh-6* mutants.** WT hermaphrodite mated to *alh-6;gst-4p::gfp* males fed OP50 supplemented with 2.5mM riboflavin results in increase in total brood size compared to non-supplemented *alh-6;gst-4p::gfp* males. *, p<0.05; **, p<0.01; ***, p<0.001; ****, p<0.0001. All studies performed in biological triplicate; refer to Table S1 for n for each comparison.

**Figure S8. *prdh-1* mutation is causal for suppression of increased SKN-1 activity in *alh-6*.** (a) Day 3 adult *alh-6;gst-4p::gfp* fed L4440 (control RNAi) are bright green on the muscle. B) Day 3 adult *alh-6;gst-4p::gfp* fed *prdh-1* RNAi are dim green on the muscle.

**Figure S9. *prdh-1* activity is required for sperm-specific fertility defects in *alh-6* mutants.** (a-c) *prdh-1* mutation rescues reduced brood size and increased number of unfertilized oocytes (a), reduced sperm number (b), and sperm competition (b) in *alh-6* animals. *gst-4p::gfp* reporter strains were used for a and c. Comparisons of A was done using ANOVA. All studies performed in biological triplicate; refer to Table S1 for n for each comparison.

**Figure S10. Dietary supplement of antioxidant NAC does not impact sperm function in wild type or *prdh-1* mutants.** Dietary supplementation of 5mM NAC does not affect WT sperm size (a) or sperm activation (b). Dietary NAC supplementation does not alter *prdh-1;alh-6* sperm size (c) or sperm activation

(d). Comparisons of groups are done in using ANOVA. Comparisons of sperm activation are done using Fisher's exact test with adjusted p-value cutoffs. *, $p<0.05$; **, $p<0.01$; ***, $p<0.001$; ****, $p<0.0001$. All studies performed in biological triplicate; refer to Table S1 for n for each comparison.

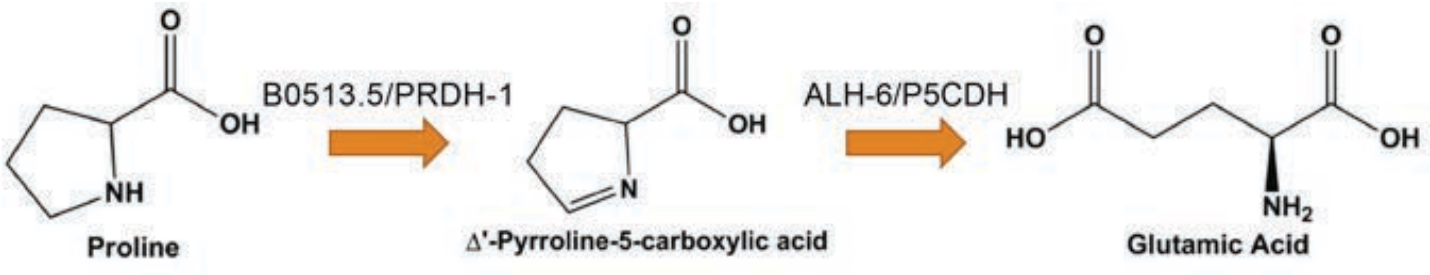


Supplemental Figure 1

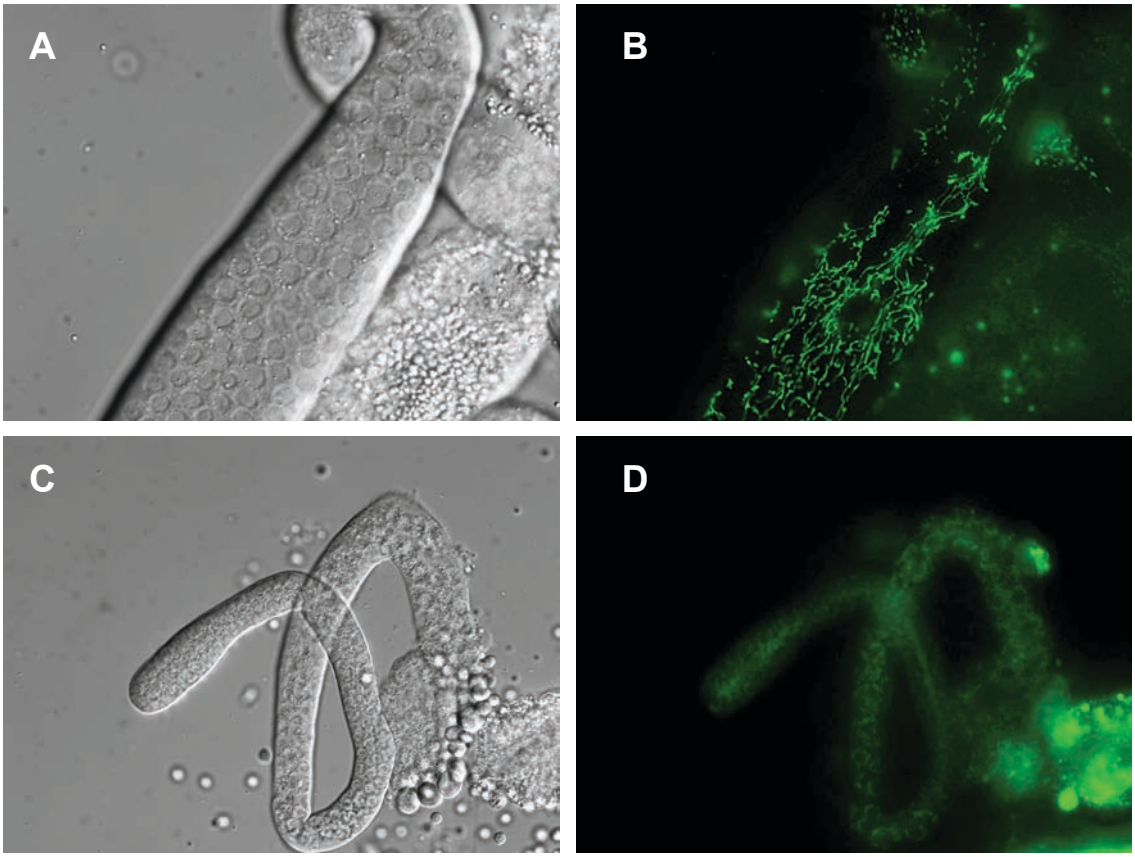


Supplemental Figure 2

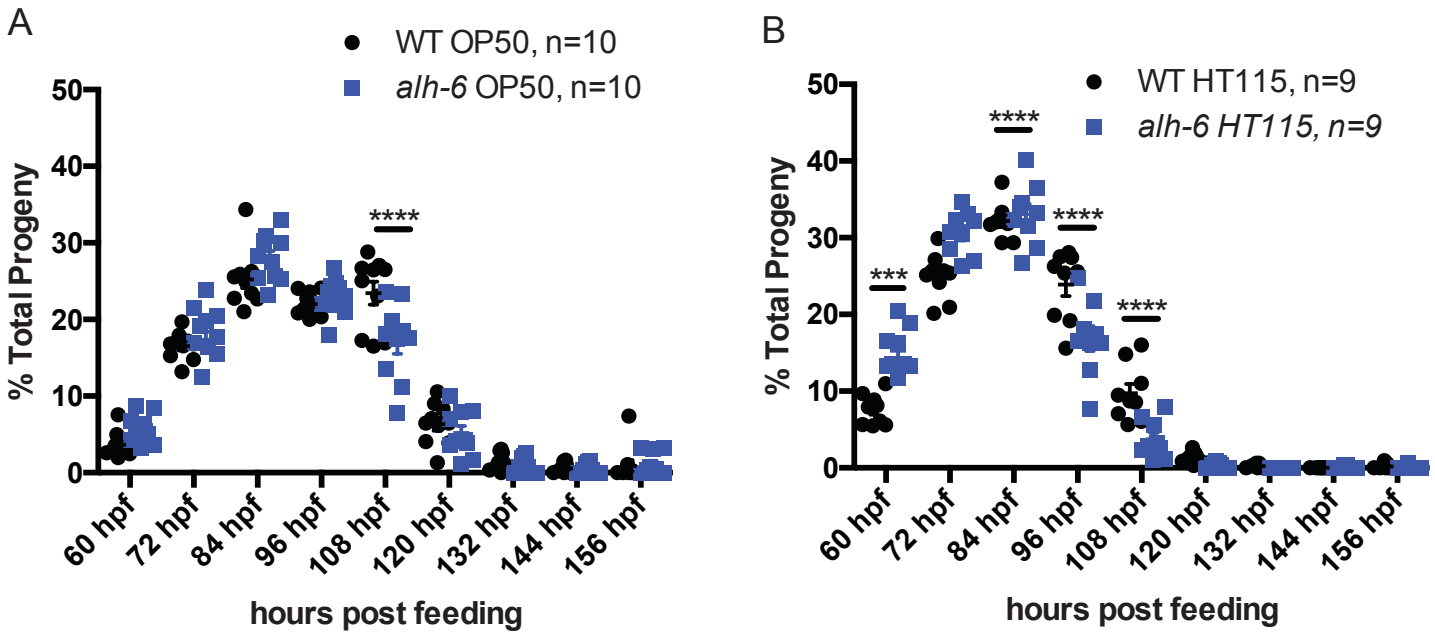


Supplemental Figure 3

A

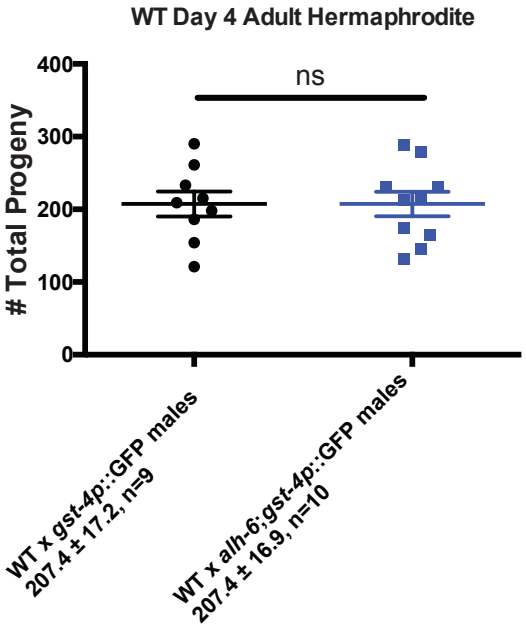


B

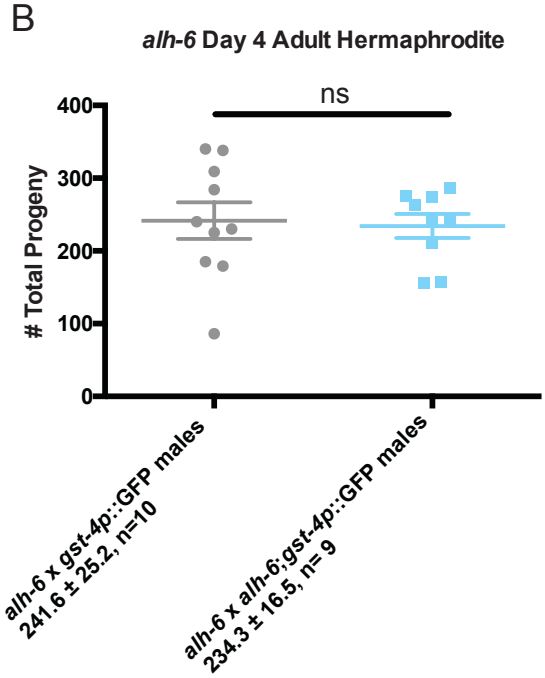


Supplemental Figure 4

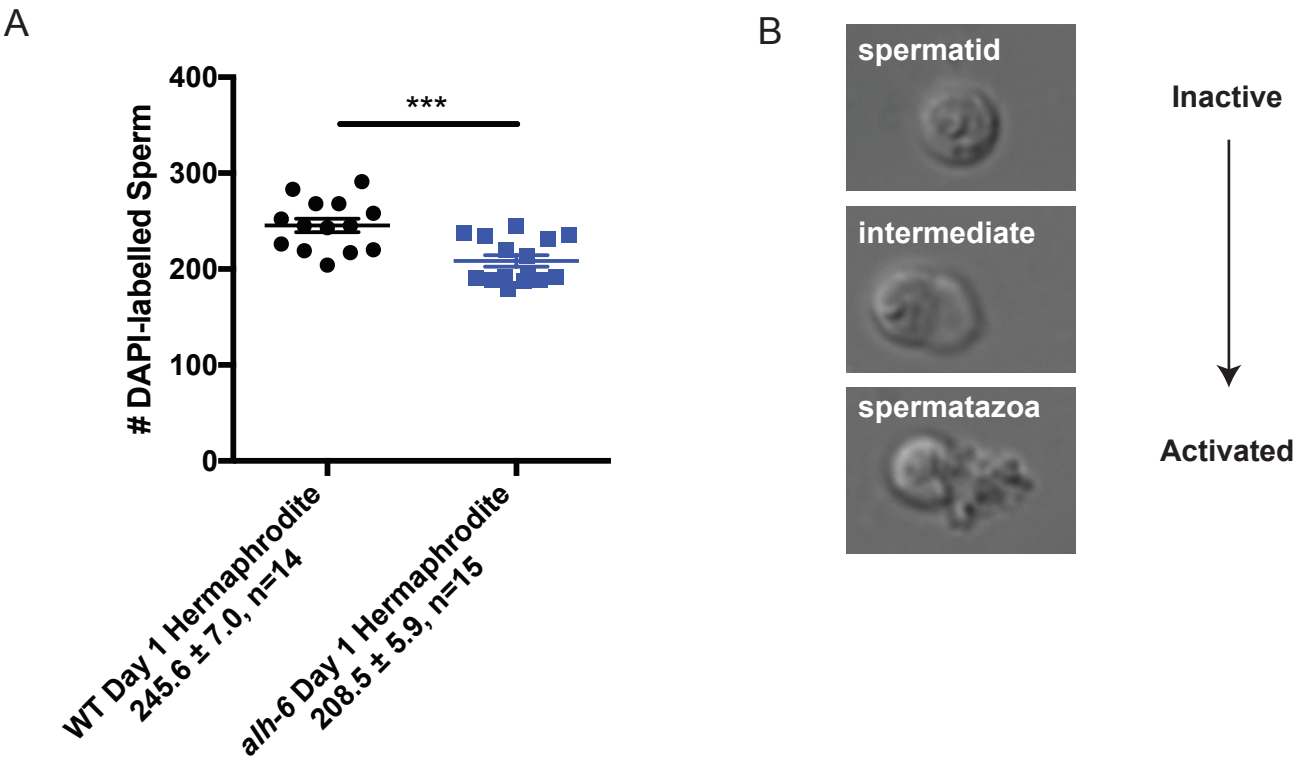


Supplemental Figure 5

A

*alh-6(lax105)* vs wild type
2-fold increase in expression (0.05 FDR)

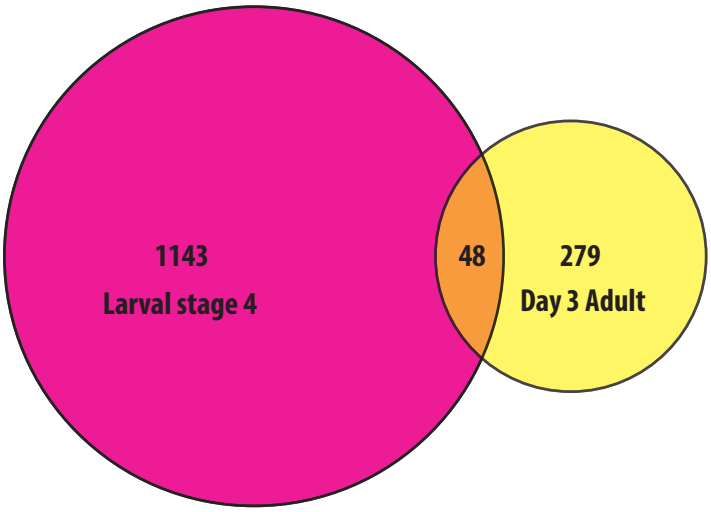


B

*alh-6(lax105)* vs wild type
2-fold decrease in expression (0.05 FDR)

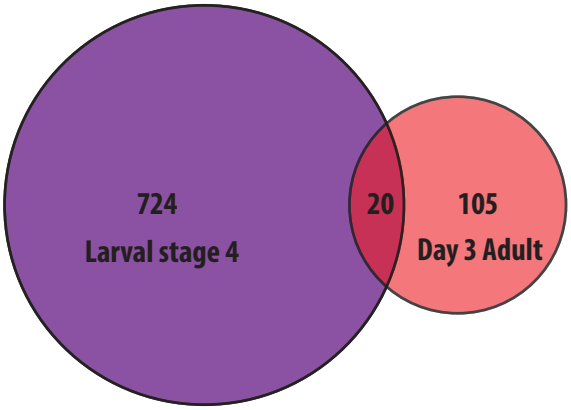


Supplemental Figure 6

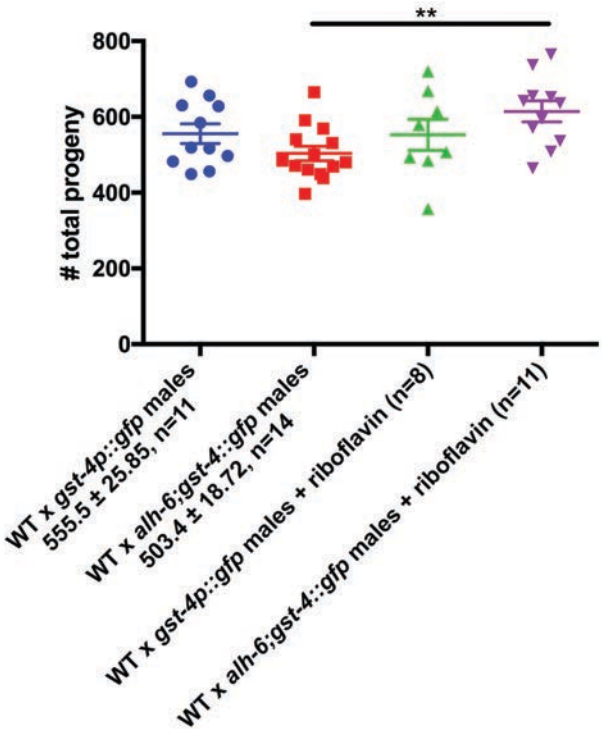


Supplemental Figure 7

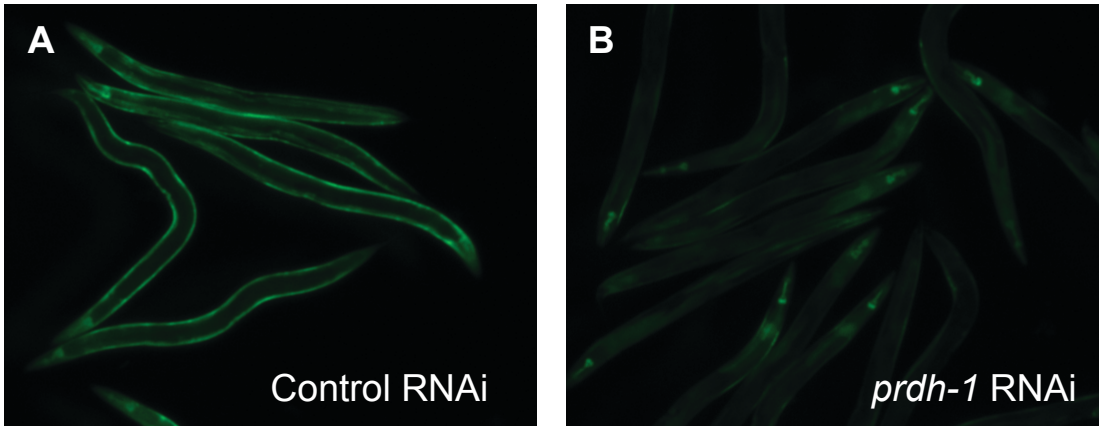


Supplemental Figure 8

A

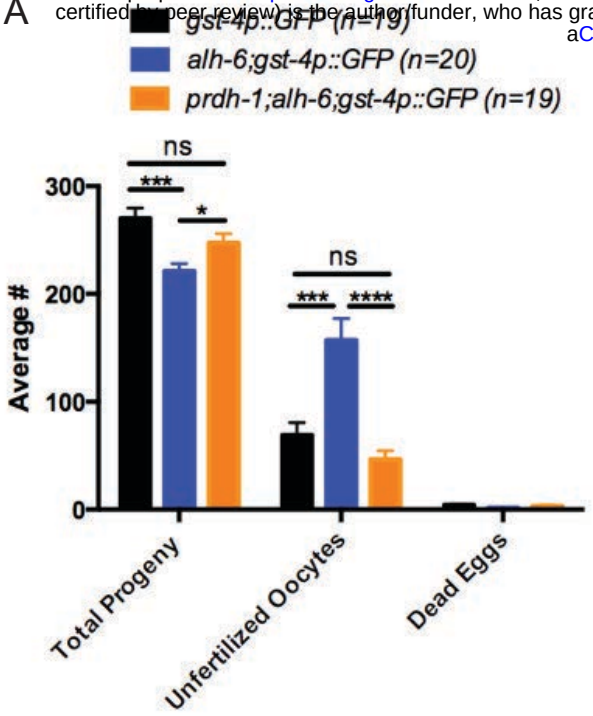


B

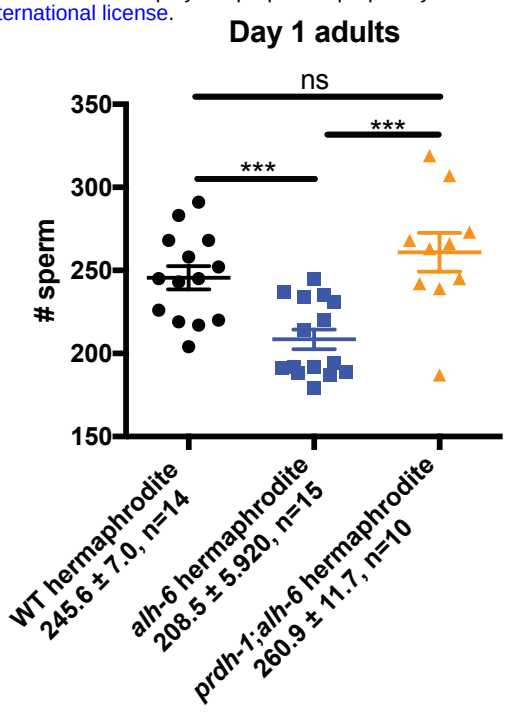


C

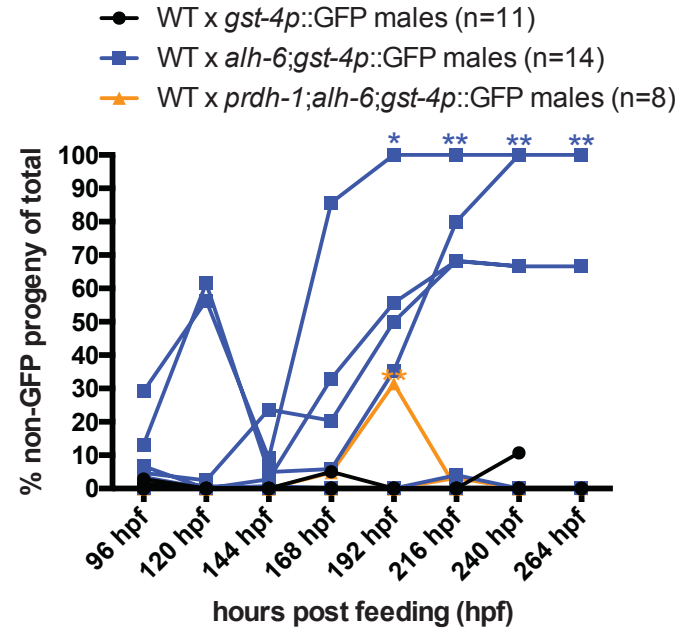


Supplemental Figure 9

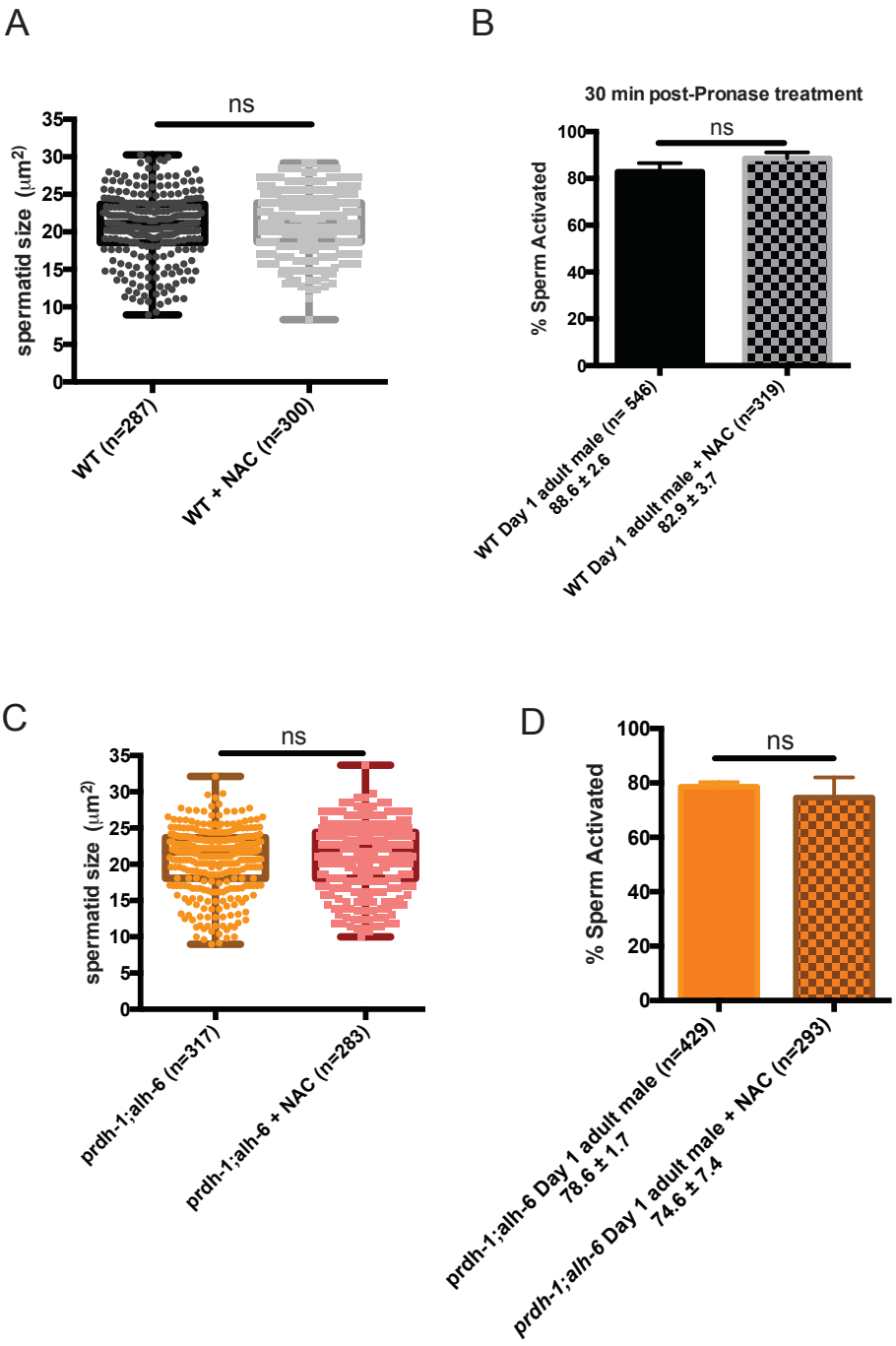


Supplemental Figure 10

| | | | | | | | |
|---|---|---|---|---|---|---|---|
| **Fig 1A** | **WT** | | ***alh-6*** | | | | |
| | | 17 | | 18 | | | |
| **Fig 1B** | **WT** | | ***alh-6*** | | | | |
| | | 9 | | 9 | | | |
| **Fig 1C** | ***gst-4p::gfp*** | | ***alh-6;gst-4p::gfp*** | | | | |
| | | 19 | | 20 | | | |
| **Fig 1D** | **WT x WT males** | | ***alh-6* x WT males** | | | | |
| | | 12 | | 12 | | | |
| **Fig 1E** | **WT x *gst-4p::gfp* males** | | ***WT* x *alh-6;gst-4p::gfp* males** | | | | |
| | | 11 | | 14 | | | |
| **Fig 2A** | **WT** | | ***alh-6*** | | | | |
| | | 23 | | 25 | | | |
| **Fig 2B** | **WT** | | ***alh-6*** | | | | |
| | | 287 | | 297 | | | |
| **Fig 2C** | **WT** | | ***alh-6*** | | | | |
| | | 546 | | 555 | | | |
| **Fig 3A** | **WT - L4** | | ***alh-6* - L4** | | **WT - Day 3** | | ***alh-6* - Day 3** |
| 4000 worms each | | 3 | | 3 | 3 | | 3 |
| **Fig 4B** | **WT - L4** | | ***alh-6* - L4** | | **WT - Day 3** | | ***alh-6* - Day 3** |
| 3000-5000 worms each | | 8 | | 9 | 3 | | 3 |
| **Fig 4C** | **WT** | | ***alh-6*** | | ***alh-6* + riboflavin** | | |
| | | 287 | | 297 | 323 | | |
| **Fig 4C** | **WT** | | ***alh-6*** | | ***alh-6* + riboflavin** | | |
| | | 546 | | 555 | 353 | | |
| **Fig 5C** | **WT - L4** | | ***alh-6* - L4** | | **WT - Day 3** | | ***alh-6* - Day 3** |
| 4000 worms each | | 3 | | 3 | 3 | | 3 |
| **Fig 5D** | **WT** | | ***alh-6*** | | ***prdh-1;alh-6*** | | ***alh-6* + NAC** |
| | | 287 | | 297 | 317 | | 322 |
| **Fig 5E** | **WT** | | ***alh-6*** | | ***prdh-1;alh-6*** | | ***alh-6* + NAC** |
| | | 546 | | 555 | 429 | | 435 |
| **Fig 6G** | **WT** | | ***alh-6*** | | ***prdh-1;alh-6*** | | |
| | | 37 | | 46 | 60 | | |
| **Fig 6H** | **WT** | | ***alh-6*** | | ***alh-6* + NAC** | | |
| | | 29 | | 49 | 56 | | |
| **Fig 6I** | **WT** | | ***alh-6*** | | | | |

| | | | | | | | |
|---|---|---|---|---|---|---|---|
| | | 38 | | 32 | | | |
| **Fig 6J** | **WT L4440** | | ***alh-6* L4440** | | **WT *fzo-1* RNAi** | | ***alh-6 fzo-1* RNAi** |
| | | 103 | | 119 | | 92 | 102 |
| **Fig 6K** | **WT** | | ***alh-6*** | | ***drp-1*** | | ***alh-6;drp-1*** |
| | | 156 | | 134 | | 157 | 140 |
| **Fig 6L** | **WT L4440** | | ***alh-6* L4440** | | **WT *fzo-1* RNAi** | | ***alh-6 fzo-1* RNAi** |
| | | 303 | | 336 | | 337 | 328 |
| **Fig 6M** | **WT** | | ***alh-6*** | | ***drp-1*** | | ***alh-6;drp-1*** |
| | | 419 | | 476 | | 439 | 432 |
| **Fig S3A** | **WT** | | ***alh-6*** | | | | |
| | | 10 | | 10 | | | |
| **Fig S3B** | **WT** | | ***alh-6*** | | | | |
| | | 9 | | 9 | | | |
| **Fig S4A** | **WT x *gst-4p::gfp* males** | | ***WT* x *alh-6;gst-4p::gfp* males** | | | | |
| | | 9 | | 10 | | | |
| **Fig S4B** | ***alh-6* x *gst-4p::gfp* male** | | ***alh-6* x *alh-6;gst-4p::gfp* males** | | | | |
| | | 10 | | 9 | | | |
| **Fig S5A** | **WT** | | ***alh-6*** | | | | |
| | | 14 | | 15 | | | |
| **Fig S6** | **WT - L4** | | ***alh-6* - L4** | | **WT - Day 3** | | ***alh-6* - Day 3** |
| 4000 worms each | | 3 | | 3 | | 3 | 3 |
| **Fig S7A** | **WT - L4** | | ***alh-6* - L4** | | **WT - Day 3** | | ***alh-6* - Day 3** |
| 3000-5000 worms each | | 9 | | 9 | | 6 | 4 |
| **Fig S7B** | **WT x *gst-4p::gfp* males** | | ***WT* x *alh-6;gst-4p::gfp* males** | | **WT x *gst-4p::gfp* m** | | ***WT* x *alh-6;gst-4p::gfp* males + riboflavin** |
| | | 11 | | 14 | | 8 | 11 |
| **Fig S8** | **L4440** | | ***prdh-1* RNAi** | | | | |
| | 30-50 | | 30-50 | | | | |
| **Fig S9A** | ***gst-4p::gfp*** | | ***alh-6;gst-4p::gfp*** | | ***prdh-1;alh-6;gst-4p::gfp*** | | |
| | | 19 | | 20 | | 19 | |
| **Fig S9B** | **WT** | | ***alh-6*** | | ***prdh-1;alh-6*** | | |
| | | 14 | | 15 | | 10 | |
| **Fig S9C** | **WT x *gst-4p::gfp* males** | | ***WT* x *alh-6;gst-4p::gfp* males** | | **WT x *prdh-1;alh-6;gst-4p::gfp* males** | | |
| | | 11 | | 14 | | 8 | |
| **Fig S10A** | **WT** | | **WT + NAC** | | | | |
| | | 287 | | 300 | | | |

| | | | | |
|---|---|---|---|---|
| **Fig S10B** | **WT** | | **WT + NAC** | |
| | | 546 | | 319 |
| **Fig S10C** | ***prdh-1;alh-6*** | | ***prdh-1;alh-6* + NAC** | |
| | | 317 | | 283 |
| **Fig S10D** | ***prdh-1;alh-6*** | | ***prdh-1;alh-6* + NAC** | |
| | | 429 | | 293 |